EFFECTIVE INTERACTIONS AND ENERGY FUNCTIONALS: APPLICATIONS TO NUCLEAR SYSTEMS

MARCELLA GRASSO

Institut de Physique Nucléaire
IN2P3-CNRS, Université Paris-Sud
91406 Orsay Cedex, France

ABSTRACT
An overview of mean-field-based and beyond-mean-field approaches is presented in the framework of the Energy Density Functional with a special attention paid to Skyrme functionals. Differences and commont points between the Energy Density Functional Theory and the Density Functional Theory are underlined.
Applications to nuclei and neutron stars are shown. Nuclear matter properties are also analyzed in the context of the Energy Density Functional: isospin effects and spin instabilities are discussed.
Finally, the predictive power of Energy Density Functional models is addressed.

I – INTRODUCTION

The description of many-body systems is one of the most difficult problems in physics owing to the huge number of degrees of freedom which are involved. Many-body methods and techniques constitute an interdisciplinary domain which relates several fields such as nuclear physics, solid state physics, atomic physics and quantum chemistry [FW71, Ma67, RS80].

Nuclei are quantum many-body systems presenting a wide and diversified spectrum of properties. The rich phenomenology associated to nuclear systems is related to the complexness of the nuclear many-body problem. When attacking this problem from a theoretical point of view two main concerns have to be addressed: i) the way to deal with the nuclear interaction; ii) the choice of the degrees of freedom to explicitely take into account in the model in order to describe the phenomenon of interest. These two aspects are strictly related one to the other.
As far as the interaction is concerned, in parallel with the traditional ways to deal with this issue (namely, the development of realistic and phenomenological effective interactions) new trends and perspectives are being explored nowadays aiming at introducing the nuclear interaction in a more fundamental way (see Lectures of E. Epelbaum and Th. Duguet). In this respect, the links with the underlying theory of quantum chromo-dynamics (QCD) are analyzed and used through the introduction of effective field theories [Bo01, Bo-

1-03, Bo-2-03, Ep09]. This modern and very promising way to deal with the nuclear interaction will certainly provide a deeper and wider comprehension of its properties. However, the investigations based on more conventional approaches have certainly to be pursued and developed in a complementary way so that the two frameworks can enrich each other in the coming years.
As far as the phenomenological effective interactions are concerned, an important advantage in choosing them is that they can be easily used in quite sophisticated mean-field and beyond-mean-field methods. The concern of using sophisticated beyond-mean-field models is crucial especially within the perspectives of describing the properties of weakly bound exotic nuclei. Indeed, in the exotic regions of the nuclear chart new and complex phenomena may manifest and a proper treatment of correlations within beyond-mean-field models may become necessary.
In nuclear physics, the phenomenological interactions which are currently used in a non-relativistic framework are of Skyrme [Sk56, Sk59] (zero-range) and Gogny [Go75] (finite-range with Gaussians) type. By applying the variational procedure to construct the mean field, phenomenological density functionals can be derived starting from these interactions. These functionals and the theoretical models which typically employ them constitute a formal framework known as the Energy Density Functional (EDF) theory.
It is worth mentioning that also in the case of relativistic formulations several investigations are concentrated on the analysis of the functionals EDF, derived in this context from a Lagrangian and not from an interaction (see, for instance, Ref. [Ni08]). Relativistic EDF models inspired by low-energy QCD have also been recently proposed [Fi03, Fi04, Fi06, Fi07].

In last years, new trends have started being explored aiming at connecting the EDF framework to that of the Density Functional Theory (DFT) which is widely diffused and currently used in solid state physics and chemistry to evaluate, for instance, band structure in solids and binding energies in molecules [DR90, Ko06]. Some examples of these bridges that are being constructed can be found in Refs. [Be-1-09, Be-2-09, Do07, Du09, En07, Gi-1-08, Gi-2-08, Ko08, La09, Me09] and essentially concern two types of investigations: i) extensions of the DFT theorems to the nuclear case; ii) work on the functionals to understand which are the best forms and parameters to describe a large number of nuclei. In this respect, a reflection around the eventual inclusion of correlations in the functionals is pursued by the community and different issues are debated: for instance, one crucial point in the debate is whether the correlations related to the collective behavior or the dynamical degrees of freedom should also be taken into account in the functionals.

In this manuscript, we first address the features of the two theoretical frameworks DFT and EDF. As far as EDF is concerned, we deal only with non-relativistic models. Links and differences between the two theories EDF and DFT are discussed and some examples of EDF mean-field-based and beyond-mean-field models are presented. In the manuscript, 'beyond mean field' means that correlations are explicitely included in the theoretical framework in order to go beyond the mean-field description which is typically based on the use of an uncorrelated ground state. Due to the limited available space, the list of the shown examples and of the beyond-mean-field methods which we are going to mention and illustrate is far from being exhaustive. We have made a selection of topics and, following this selection, some extensions of the mean-field approach within the EDF framework will be explored.

The manuscript is organized as follows: In Sec. II the independent-particle approximation on which the DFT and the EDF are based is discussed.
An introduction to some basic topics of the DFT is provided in Sec. III.
The most used phenomenological interactions and the associated energy density functionals (derived with the variational mean-field procedure in the framework of the

EDF) are introduced in Sec. IV, while some applications of the EDF models are shown in Sec. V. The role of correlations and isospin effects are discussed and the importance of going beyond-mean-field is commented in some cases, especially within the perspective of analyzing exotic nuclei.
To conclude this part, differences and common points between DFT and EDF are summarized in Sec. VI.
A first kind of correlations, namely pairing correlations (owing to the formation of Cooper pairs in some open-shell nuclei) and the associated model Hartree-Fock-Bogoliubov (HFB) are introduced in Sec. VII. This model is a first natural extension of the mean field Hartree-Fock (HF) approach where the existence of Cooper pairs is modelled by the introduction of the concept of quasiparticles through the unitary Bogoliubov transformations. Different strategies to choose the pairing interaction can be followed and this is discussed in the second part of Sec. VII.
From the small-amplitude limit of the time-dependent (TD) mean-field approach, TDHF(B), the (quasiparicle) random-phase approximation ((Q)RPA) equations can be derived in which collectivity is taken into account providing a way to deal with the coherent motion of nucleons in the system (Sec. VIII). The small-amplitude approximation which is adopted to derive the (Q)RPA equations allows one to describe only a limited class of dynamical features, namely, the small-amplitude oscillations around the ground state density.
A way to go beyond mean-field models may be performed by coupling individual and collective degrees of freedom. This aspect is detailed in Sec. IX where the particle-vibration coupling and the second RPA (SRPA) are introduced. In other beyond-mean-field models an explicitely correlated ground state is used: these models are based on extensions of the RPA (Sec. X). If the use of a correlated ground state is performed together with the coupling between individual and collective behavior, other beyond-mean-field methods can be derived such as, for instance, the Generator Coordinate Method (GCM) or the variational multiparticle-multihole configuration mixing (also described in Sec. X).
A scheme about how the topics which constitute the first ten sections of the manuscript are organized is displayed in Fig. 1 where the connections among all these topics are also shown.

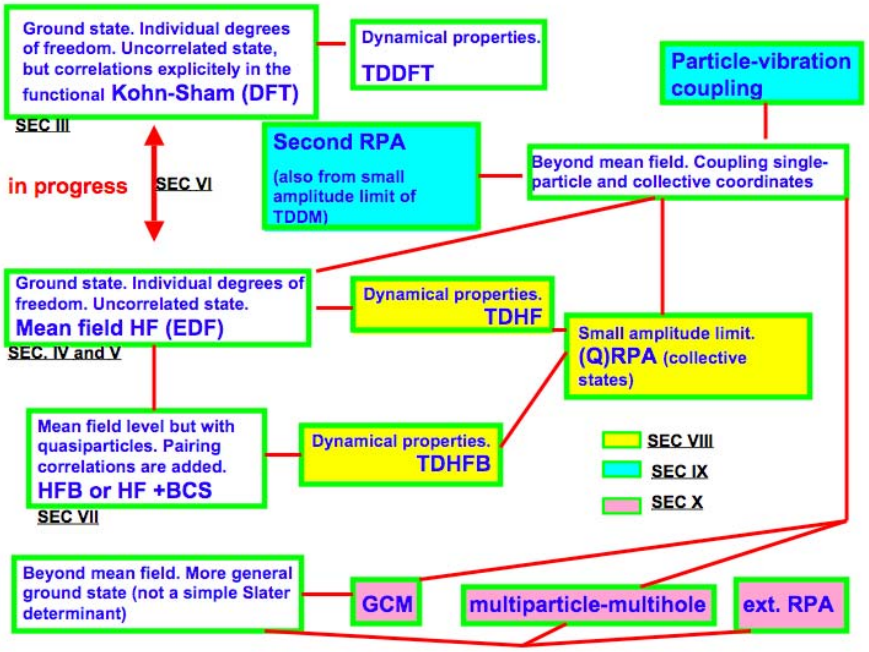

Fig. 1

Scheme about the formal aspects developed in the manuscript and connections among them

Sec. XI is devoted to a brief presentation of nuclear astrophysics topics and in particular to neutron stars. Some applications of the EDF models in this framework are shown. A more detailed description of this topic can be found in the Lectures of P. Pizzochero.
Finally, nuclear matter properties analyzed within the EDF are discussed in Sec. XII. Isospin effects in asymmetric matter and the presence of instabilities are briefly addressed. This topic and its experimental implications are presented in detail in the Lectures of M.-F. Rivet.
As a conclusion, the EDF-models predictive power is discussed in Sec. XIII and this analysis opens several directions for perspectives.

II – THE NUCLEAR MANY-BODY PROBLEM. THE INDEPENDENT-PARTICLE APPROXIMATION

The solution of the many-body Schrödinger equation cannot be performed exactly owing to the huge number of degrees of freedom which are typically involved in a many-body problem. Procedures to simplify the problem must be used and a classification of the relevant degrees of freedom must be performed. According to the typical energy and length scales of the system, to the phenomenon under study and to the used theoretical tool, some degrees of freedom may be considered more important than others (which can be neglected or eventually included in an effective way). In some cases, a special separation of scales may be performed which allows one to treat in a full quantum way only some degrees of freedom and to deal with the others with a semiclassical approximation.
The many-body Hamiltonian in second quantization is given by the following expression:

$$H = \sum_{\alpha\beta} \langle \alpha | T | \beta \rangle a_\alpha^+ a_\beta + \frac{1}{2} \sum_{\alpha\beta\gamma\delta} \langle \alpha\beta | V | \gamma\delta \rangle a_\alpha^+ a_\beta^+ a_\delta a_\gamma + \ldots . \quad (1)$$

The first term describes the kinetic contribution plus an eventual external potential and the second term, which is a two-body term, represents the interaction among the constituents. In the context of the nuclear EDF, the degrees of freedom which are explicitely taken into account to deal with the many-body problem are the nucleons. Protons and neutrons are thus the A constituents of the system. Three-, four-, ... A-body contributions to the interaction are often neglected in the Hamiltonian and have not been explicitely written in Eq. (1).
One of the current approximations used to simplify the Schrödinger equation associated to the Hamiltonian, Eq. (1), is the so-called independent-particle approximation on which, for instance, both the mean field and the shell model are based. This approximation is valid when the system under study is dilute in the sense that the mean free path of its constituents is comparable with or larger than the typical length scale of the system. Due to the combination of the Pauli and the uncertainty principles, nuclei satisfy this property. Hence, one can imagine to treat each nucleon of the system as independent of the others and to introduce the interaction among the particles through a single-particle effective potential which describes on average the action of all the other particles on the single constituent. This effective potential, constructed by all the particles, can be viewed as an external potential. Within this picture, the system is equivalent to that of non-interacting particles in an external potential.

III – A SHORT INTRODUCTION TO THE DENSITY FUNCTIONAL THEORY

The DFT is based on very general concepts and theorems and this explains its huge diffusion and easy applicability to many domains [Ca06, Dr90, Fio03, Ma92, Pa89].
This theory has been introduced to describe the properties of many-electron systems. It has been founded in the 60s with the formulation of the Hohenberg-Kohn (HK) theorem [HK64] and the introduction of the Kohn-Sham (KS) equations [KS65]. The KS equations provided a practical way to replace the minimization procedure implied by the HK theorem with the solution of an effective Schrödinger equation for a system of non-interacting particles. This means that the KS equations are based on the independent-particle approximation described in the previous section: the many-body problem is reduced to a one-body effective problem (where, however, correlations are actually included). In 1998 the Nobel Prize for chemistry was attributed to W. Kohn, the father of the DFT, and to J. Pople for his important contribution in the numerical implementations of the DFT in computational chemistry.
The procedure which is usually followed to treat a problem in quantum physics (i.e., first solving the Schrödinger equation with a given potential, getting a wave function and constructing with it the mean values of the operators, for instance, the density) is inverted in the DFT. The density plays a fundamental role in this theory and it is the starting point of the procedure. The knowledge of the density allows to evaluate the wave function and thus the potential.
To develop this framework, functionals are used, which are functions of functions. Functional variations and derivatives are introduced as mathematical tools for the development of the theory.
In the nest subsections, we present some aspects of the DFT following the Introduction to the DFT proposed in Ref. [Ca06].

Content of the Hohenberg-Kohn theorem

Let us consider a system of N interacting particles in an external potential. The many-body Hamiltonian is:

$$\left[\sum_{i=1}^{N}\left(-\frac{\hbar^2\nabla_i^2}{2m}+v(\vec{r}_i)\right)+\sum_{i<j}U(\vec{r}_i,\vec{r}_j)\right]\Psi(\vec{r}_1,\vec{r}_2,...,\vec{r}_N)=E\Psi(\vec{r}_1,\vec{r}_2,...,\vec{r}_N), \quad (2)$$

where U is the interaction and v the external potential.
If the ground state density ρ_0 is known, it is possible to determine, starting from this density, the external potential (up to an additive constant) and the ground state wave function Ψ_0.
The non degenerate ground state wave function is a unique functional of the ground state density ρ_0:

$$\Psi_0(\vec{r}_1,...,\vec{r}_N)=\Psi[\rho_0(\vec{r})]. \quad (3)$$

Consequently, the expectation value of any observable in the ground state is a functional of ρ_0:

$$O_0=\langle\Psi[\rho_0]|\hat{O}|\Psi[\rho_0]\rangle=O[\rho_0]. \quad (4)$$

This means that also the ground state energy is a functional of ρ_0.
For each external potential v, a functional $E_v[\rho]$ exists which is minimized by ρ_0. The ground state energy E_0 is equal to $E_v[\rho_0]$. This variational property may be written as:

$E_v[\rho_0] \leq E_v[\rho]$ if $\rho \neq \rho_0$

and is often called the second Hohenberg-Kohn theorem.
All the other extrema of the functional correspond to physical densities (of excited states), but the excited states found in this way do not necessarily cover the whole spectrum of the Hamiltonian.
If the ground state is degenerate, a unique functional $\Psi[\rho]$ does not exist because different wave functions are associated to the same density, but a unique functional $E[\rho]$ still exists even in this case.
The HK theorem was originally proven by contradiction in the article of 1964: one assumes that the ground state wave function is not uniquely determined by ρ_0 and shows that this hypothesis leads to a contradiction with the variational principle. Alternative proofs of the theorem have been proposed later.
Within the HK theorem, the many-body problem to determine the ground state of a system may be solved by an energy minimization. A practical way to deal with this energy minimization is provided by the KS equations [KS65]: the energy minimization procedure is replaced by the solution of a Schrödinger equation for non-interacting particles. This procedure reduces the many-body problem into an effective one-body problem.

Kohn-Sham equations

The energy E, which is a functional of the density, may be written as:

$$E[\rho]=T[\rho]+U[\rho]+V[\rho], \quad (5)$$

where T is the kinetic contribution to the functional, U the interaction term and V the functional related to the external potential,

$$V[\rho] = \int d^3\vec{r}\rho(\vec{r})v(\vec{r}).$$

For the kinetic part:

$$T[\rho] = T_S[\rho] + T_C[\rho], \quad (6)$$

where $T_S[\rho]$ is the mean value of the operator $\hat{T}$ calculated with the Slater determinant associated to the density. Since the wave function is a Slater determinant, the exchange contribution is fully taken into account. Hence, the term T_C contains only contributions coming from correlations. If φ are the orbitals composing the Slater determinant, T_S is written as:

$$T_S = -\frac{\hbar^2}{2m}\sum_{i=1}^{N}\int d^3\vec{r}\varphi_i^*(\vec{r})\nabla^2\varphi_i(\vec{r}). \quad (7)$$

All the functions φ are functionals of ρ (HK theorem). Thus:

$$T_S[\rho] = T_S[\{\varphi_i[\rho]\}]. \quad (8)$$

The exact functional is written as:

$$E[\rho] = T_S[\{\varphi_i[\rho]\}] + U_{Hartree}[\rho] + E_{xc}[\rho] + V[\rho]. \quad (9)$$

E_{XC} contains the differences $T-T_S$ and $U-U_{Hartree}$ (these terms are typically much less important than T_S and $U_{Hartree}$). The functional E_{XC} is unknown (the HK theorem garanties only that it exists). It is called exchange-correlation term and is often written as the explicit sum of an exchange term E_X and a correlation term E_C. Approximations have to be used to write the exchange-correlation term (in extensions of the DFT the exchange term is sometimes treated exactly but the correlation term is always approximated).
The minimization generating the KS equations is:

$$0 = \frac{\delta E[\rho]}{\delta\rho(\vec{r})} = \frac{\delta T_S[\rho]}{\delta\rho(\vec{r})} + \frac{\delta V[\rho]}{\delta\rho(\vec{r})} + \frac{\delta U_{Hartree}[\rho]}{\delta\rho(\vec{r})} + \frac{\delta E_{xc}[\rho]}{\delta\rho(\vec{r})}$$

$$= \frac{\delta T_S[\rho]}{\delta\rho(\vec{r})} + v(\vec{r}) + v_{Hartree}(\vec{r}) + v_{xc}(\vec{r}). \quad (10)$$

It is worth noticing that $\frac{\delta E_{xc}}{\delta\rho}$ can be explicitely evaluated only when an approximation for E_{XC} is chosen.
For a system of non-interacting particles in an external potential v_S the minimization condition does not contain the Hartree and the exchange-correlation terms:

$$0 = \frac{\delta E[\rho]}{\delta\rho(\vec{r})} = \frac{\delta T_S[\rho]}{\delta\rho(\vec{r})} + \frac{\delta V_S[\rho]}{\delta\rho(\vec{r})} = \frac{\delta T_S[\rho]}{\delta\rho(\vec{r})} + v_S(\vec{r}). \quad (11)$$

By comparing eqs. (10) and (11) one concludes that the two minimizations provide the same result if

$$v_S(\vec{r}) = v(\vec{r}) + v_{Hartree}(\vec{r}) + v_{xc}(\vec{r}) . \quad (12)$$

The Schroedinger equation to solve is:

$$\left[-\frac{\hbar^2 \nabla^2}{2m} + v_S(\vec{r}) \right] \varphi_i(\vec{r}) = \varepsilon_i \varphi_i(\vec{r}), \quad (13)$$

Where v_s is given by eq. (12) and ε are the constraints related to the minimization procedure. With the solution of eq. (13) the density can be constructed:

$$\rho(\vec{r}) = \sum_{i=1}^{N} f_i |\varphi_i(\vec{r})|^2 , \quad (14)$$

where the coefficients f are the occupation numbers of each state. Eqs. (12) - (14) are the non-linear KS equations. They are solved iteratively up to the determination of the self-consistent solution. Thus, the KS model looks like a mean-field theory with a self-consistent effective one-body Schroedinger equation for the KS states but includes correlation effects on the ground-state density and total energy.
It is important noticing that only the density and the total energy have a physical meaning in the KS problem. The single-particle energies which are found as a solution of the KS equations do not really correspond to the physical single-particle states.
But how to solve in practice the KS equations, how to choose a form for the unknown functional E_{XC}? This is an important and delicate point since in the exchange-correlation functional all the many-body physics is contained. As already mentioned, the exchange part can be written and treated exactly. To choose a form for the correlation part different strategies may be followed: perturbation theory was used in the first applications of the DFT while Quantum Monte Carlo calculations are currently employed nowadays for electronic systems. The local-density approximation (LDA) is adopted and, in the most sophisticated functionals, gradient-corrections with derivatives of the densities are added to implement the LDA and include finite-size effects (see, e.g., [Fio03, Pe96]). Other sophisticated examples of functionals may be found in Ref. [Pe05].

IV – A MORE FAMILIAR FRAMEWORK IN NUCLEAR PHYSICS. THE ENERGY DENSITY FUNCTIONAL (FROM A PHENOMENOLOGICAL INTERACTION)

Energy density functionals are very well known and currently employed in nuclear physics since several decades. In the non-relativistic case, they are derived from effective phenomenological interactions by applying the variational principle in the framework of the mean-field approach.
While the DFT was introduced in the 60s, the Hartree-Fock (HF) mean field method was formulated in the 20s. As for the case of the DFT, the first applications have been performed for electronic systems.
The HF mean-field model is based on the independent-particle approximation. This means that the many-body Hamiltonian is approximated by an effective one-body Hamiltonian. What is neglected with this approximation is called residual interaction. The ground state is chosen as a Slater determinant, i.e.,

$$\left|\mathrm{HF}\right\rangle = \prod_{i=1}^{N} a_i^{+}\left|-\right\rangle . \qquad (15)$$

The derivation of the HF equations may be found in all many-body textbooks (see, for instance, [FW71, RS80]). The ground state wave function is determined in a variational way by a minimization of the energy:

$$E_{HF} = \frac{\left\langle \mathrm{HF}\middle|\mathrm{H}\middle|\mathrm{HF}\right\rangle}{\left\langle \mathrm{HF}\middle|\mathrm{HF}\right\rangle} . \qquad (16)$$

This corresponds to solve the Dyson equation for the one-body Green's function:

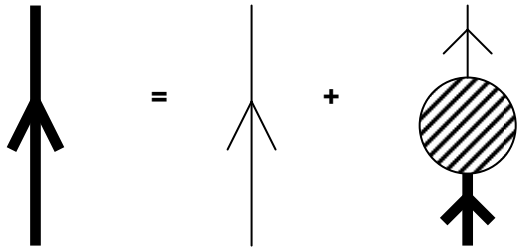

with the following approximation for the proper self-energy (first order):

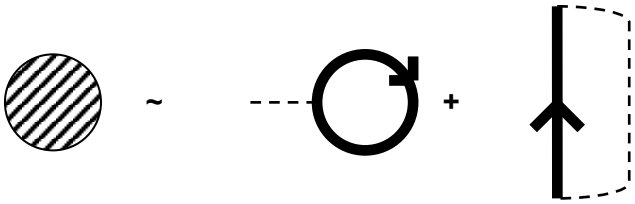

In the above diagrams, the solid thin (thick) lines represent the unperturbed or free (exact) Green's function and the dashed lines represent the interaction. The two terms in the diagram for the proper self-energy are its direct and exchange contributions. For the details about the perturbative expansion (in the interaction V) and the diagrammatic representation of the one-body Green's function, see Ref. [FW71]. The Dyson equation with the above approximation for the proper self-energy, i.e., the HF equations, can be explicitely written as:

$$\left\{-\frac{\hbar^2}{2m}\Delta + \Gamma_H(\vec{r})\right\}\varphi_k(\vec{r}) + \int d\vec{r}\,'\,\Gamma_{Ex}(\vec{r},\vec{r}\,')\varphi_k(\vec{r}\,') = \varepsilon_k\varphi_k(\vec{r}) , \qquad (17)$$

where:

$$\Gamma_H(\vec{r}) = \int d\vec{r}\,'\, v(\vec{r},\vec{r}\,')\rho(\vec{r}\,') , \qquad (18)$$

$$\Gamma_{Ex}(\vec{r},\vec{r}\,') = -v(\vec{r},\vec{r}\,')\rho(\vec{r},\vec{r}\,') . \qquad (19)$$

Γ_H and Γ_{Ex} are the direct and exchange potentials depending on the local and the non-local densities, respectively. When the used interaction is density-dependent, rearrangement terms also appear in the above expressions for the potential. The equations are solved iteratively up to the derivation of the self-consistent solution.

In nuclear physics, the introduction of the first phenomenological interactions allowed in the 70s to perform the first sophisticated numerical applications of the HF method [Go75, Ne82, VB72]. The most used phenomenological interactions are of Skyrme (zero-range) and Gogny (finite-range with Gaussians) type. Their parameters are fixed by a fitting procedure in order to reproduce some properties of selected spherical magic nuclei (binding energies and radii) and to provide a reasonable equation of state for nuclear matter (in some cases also for neutron matter). The Gogny interaction has a more microscopic formal content with respect to the Skyrme interaction because it has been introduced starting from a realistic G matrix. On the other hand, Negele and Vautherin [NV72] have shown in the 70s that a Hamiltonian density derived with the Density Matrix Expansion techniques (these techniques are used to deduce a phenomenological interaction starting from a realistic G matrix) is analogous to the Hamiltonian density obtained with a Skyrme interaction.

The standard forms of the Gogny and Skyrme interactions are very well known. For a detailed review of their expressions, properties and parametrizations see, for instance, Ref. [Me03].
The Gogny interaction contains a central term given by the sum of two Gaussians and two additional zero-range terms: a density-dependent term and a spin-orbit contribution,

$$V(r_1, r_2) = \sum_{i=1,2} \left[W_i + B_i P_\sigma - H_i P_\tau - M_i P_\sigma P_\tau \right] e^{\frac{-r^2}{\mu_i^2}} + t_3 (1 + x_3 P_\sigma) \left[\rho(\vec{R})\right]^\alpha \delta(\vec{r}) + i W_0 \vec{\sigma} \cdot \left[\vec{P}' \times \delta(\vec{r}) \vec{P}\right] \quad , \qquad (20)$$

with the following notation:

$$\vec{r} = \vec{r}_1 - \vec{r}_2 \,;\; \vec{R} = \frac{1}{2}(\vec{r}_1 + \vec{r}_2) \,;\; \vec{P} = \frac{1}{2i}(\nabla_1 - \nabla_2) \,;\; \vec{P}' \text{ cc of } \vec{P} \text{ acting on the left,}$$

$$P_\sigma = \frac{1}{2}(1 + \sigma_1 \cdot \sigma_2) = \begin{cases} +1 & S = 1 \\ -1 & S = 0 \end{cases} \;;\; P_\tau = \frac{1}{2}(1 + \tau_1 \cdot \tau_2) = \begin{cases} +1 & T = 1 \\ -1 & T = 0 \end{cases}$$

$$\sigma = \sigma_1 + \sigma_2 \;;\; \tau = \tau_1 + \tau_2$$

The first parametrization which has been introduced is D1 [De80] while the most used in present calculations is D1S [Be89] which has been adjusted to reproduce also fission barriers. More recently, the new parametrization D1N has been proposed where the fitting procedure has been implemented by including an adjustement on the neutron equation of state [Ch08]. A finite-range has been also introduced in the density-dependent term [Ch07]. A finite-range tensor contribution has been recently included and tested in HF calculations with a new parametrization proposed by Otsuka and collaborators [Ot06].

In the Skyrme interaction all terms are of zero-range and the finite-range and non-locality are simulated by velocity-dependent terms:

$$
\begin{aligned}
V(\vec{r}_1,\vec{r}_2) &= t_0(1+x_0P_\sigma)\delta(\vec{r}) \\
&+ \frac{1}{2}t_1(1+x_1P_\sigma)\left[\vec{P}'^2\delta(\vec{r})+\delta(\vec{r})\vec{P}^2\right]+t_2(1+x_2P_\sigma)\vec{P}'\cdot\delta(\vec{r})\vec{P} \\
&+ \frac{1}{6}t_3(1+x_3P_\sigma)\left[\rho(\vec{R})\right]^\alpha\delta(\vec{r}) \\
&+ iW_0\sigma\cdot\left[\vec{P}'\times\delta(\vec{r})\vec{P}\right]
\end{aligned}
\quad , \qquad \textbf{(21)}
$$

with the same notation as for the Gogny interaction.
Many Skyrme parametrizations exist (see, for instance, examples given in Ref. [Me03]).
Let us consider the mean value of H, eq. (16), in the case of a Skyrme interaction. This mean value is minimized in the variational procedure and can be written as:

$$\langle H\rangle = \int \aleph(\vec{r})d\vec{r}\ , \qquad \textbf{(22)}$$

where $\aleph$ is the Hamiltonian density or energy density. This Hamiltonian density is actually the energy density functional which is obtained, in the EDF case, starting from an interaction (in the non-relativistic framework). For the Skyrme interaction, the energy density functional is an algebraic function of the nucleon density ρ_q, the kinetic energy density τ_q and the spin-orbit density $\vec{J}_q$ (q stands for neutron or proton):

$$\rho_q(\vec{r}) = \sum_{i,\sigma}\left|\varphi_i(\vec{r},\sigma,q)\right|^2\ , \qquad \textbf{(23)}$$

$$\tau_q(\vec{r}) = \sum_{i,\sigma}\left|\vec{\nabla}\varphi_i(\vec{r},\sigma,q)\right|^2\ , \qquad \textbf{(24)}$$

$$\vec{J}_q(\vec{r}) = (-i)\sum_{i,\sigma,\sigma'}\varphi_i^*(\vec{r},\sigma,q)\left[\vec{\nabla}\varphi_i(\vec{r},\sigma',q)\times\langle\sigma|\vec{\sigma}|\sigma'\rangle\right], \qquad \textbf{(25)}$$

where φ are the wave functions defining the ground state Slater determinant. For a detailed derivation of the functional see, for instance, Ref. [VB72]. The sums in the above three equations are taken over all the occupied states. One can separate the following different contributions in the functional:

$$\aleph = K + \aleph_0 + \aleph_3 + \aleph_{eff} + \aleph_{fin} + \aleph_{SO} + \aleph_{sg} + \aleph_{coul}\ , \qquad \textbf{(26)}$$

where the terms in the above equation stand for the kinetic part, the contribution coming from the central part, the density-dependent contribution, the effective-mass term, the contribution coming from gradient terms, the spin-orbit coupling, the spin-gradient coupling (containing the tensor contribution) and the Coulomb contribution, respectively. The detailed expressions for each of these terms can be found in Refs. [Me03, VB72] for the case where time-reversal invariance (even-even nucleus) and spherical symmetry are assumed.
The spin-gradient term is often omitted in Skyrme mean field calculations and most of the available parametrizations have been obtained without this contribution. In the case of spherical symmetry and for an even-even nucleus the spin-orbit density is written as:

$$J_q(r) = \frac{1}{4\pi r^3}\sum_{lj}(2j+1)\left[j(j+1) - l(l+1) - \frac{3}{4}\right]\varphi^2_{lj,q}(r)\,, \qquad (27)$$

where $\varphi(r)$ are the radial parts of the wave functions. The $\aleph_{sg}$ contribution is given by:

$$\frac{1}{2}\alpha\left(J_n^2 + J_p^2\right) + \beta J_n J_p\,, \qquad (28)$$

where:

$$\alpha = \alpha_C + \alpha_T\,;\ \beta = \beta_C + \beta_T\,. \qquad (29)$$

α_C and β_C describe the central non-local contribution and can be written in terms of the other parameters of the Skyrme force,

$$\alpha_C = \frac{1}{8}(t_1 - t_2) - \frac{1}{8}(t_1 x_1 + t_2 x_2), \qquad (30)$$

$$\beta_C = -\frac{1}{8}(t_1 x_1 + t_2 x_2). \qquad (31)$$

These terms have been included in some Skyrme parametrizations like Sly5 [Ch98]; α_T and β_T are the parameters related to the tensor contribution. This contribution has been perturbatively included in some recent works on top of existing parametrizations (see, for instance, Ref. [Co07]). In a recent investigation, new global fits of all the parameters have been performed including this contribution and several sets of parameters have been introduced [Le07].
Other non-standard terms may be included in the Skyrme interaction enriching in this way the energy density functional with new contributions. An example of this will be mentioned in Sec. XII where the ferromagnetic instabilities of the Skyrme force are briefly addressed.

V – EXAMPLES OF APPLICATIONS OF THE EDF MEAN-FIELD MODELS TO NUCLEI

The ground state of nuclei can be described with mean-field EDF models in the HF approximation or within the Hartree-Fock-Bogoliubov picture for open-shell nuclei (where pairing correlations are included; see Sec. VII). We provide in this section some examples of results obtained with the Hartree-Fock-Bogoliubov model.
An observable that can be evaluated within these models is the mass, related to the total binding energy B(N,Z) of the nucleus by the relation:

$$M(N,Z) = Z\,M_p + N\,M_n - B(N,Z)$$

where M_p and M_n are the proton and neutron masses, respectively. Masses are the first observables that are measured in nuclei and constitute thus the first piece of information which can be experimentally obtained about the properties of the nucleus under study. Theoretical mean-field models can actually be judged for their ability in accurately predicting masses of nuclei. As already mentioned, masses of some spherical magic nuclei are used in the fitting procedure of the parameters of the phenomenological effective interactions.
Masses are interesting observables also from an astrophysical point of view. It is known that they are very important in r-process nucleosynthesis calculations [Ar07]. Accurate

and sophisticated Hartree-Fock-Bogoliubov mass-models have thus been elaborated for these astrophysical applications. We mention here two recent works of Goriely and collaborators where the fits of a new Skyrme and a new Gogny parametrizations have been performed; 2149 measured masses are used for the fitting procedure and, owing to this feature, the new parametrizations are expected to have a strong predictive power for masses in the unexplored regions of the nuclear chart. Figs. 2 and 3 are extracted from Refs. [Go-1-09] and [Go-2-09]. The differences between the measured [Au03] and the theoretical masses (obtained with the Gogny parametrization D1M in Fig. 2 and the Skyrme parametrization HFB-17 in Fig. 3) are represented as a function of the neutron number N.

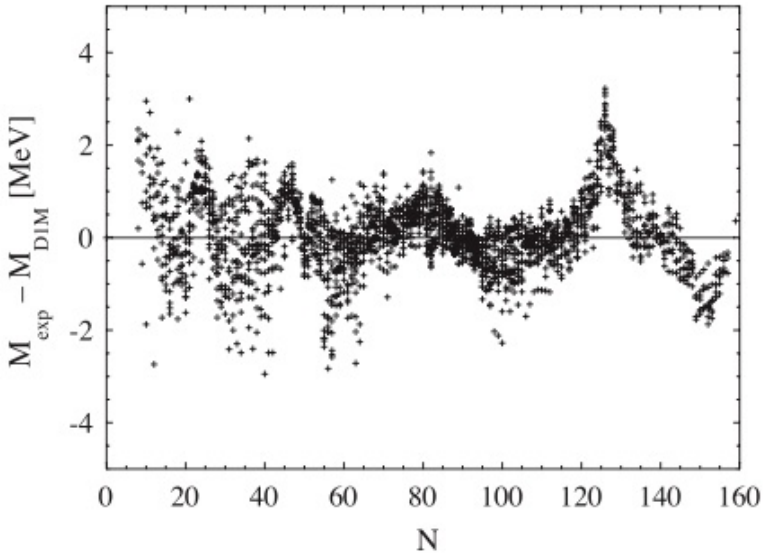

Fig. 2 [Go-1-09]

Difference between the measured [Au03] and the theoretical masses obtained with the Gogny parametrization D1M as a function of the neutron number N

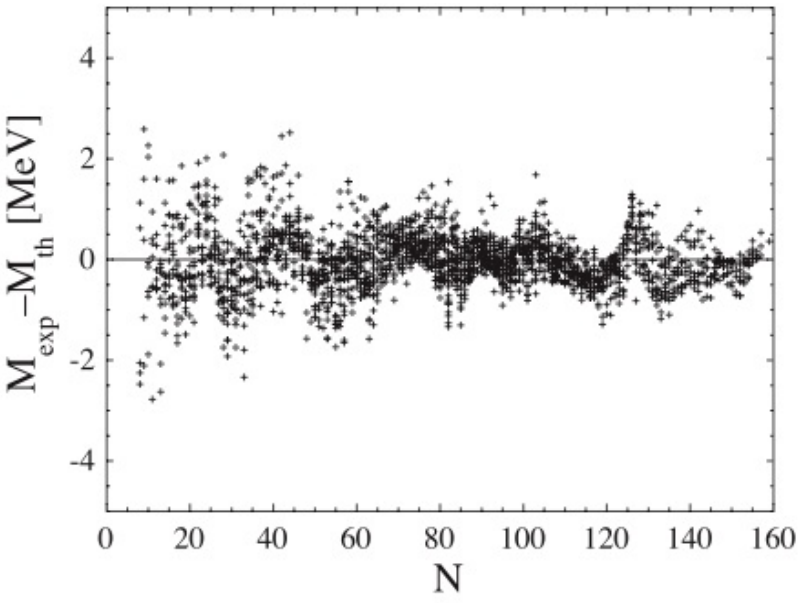

Fig. 3 [Go-2-09]

Difference between the measured [Au03] and the theoretical masses obtained with the Skyrme parametrization HFB-17 as a function of the neutron number N

The rms deviation with respect to the 2149 measured masses is equal to 798 (581) keV for the new Gogny (Skyrme) parametrization.

Knowing masses, the one- and two-nucleon separation energies S_n, S_p and S_{2n}, S_{2p} may be evaluated and the drip line positions can be predicted. Experimental data on the drip line positions are unfortunately missing except for light nuclei. Hence, the theoretical predictions essentially concern unexplored regions of the nuclear chart . This is a very delicate point since it turns out that these predictions are very strongly model dependent and this feature shows how poor in this respect is the predictive power of the available EDF models.
An example of results obtained for the two-neutron separation energies is shown in Fig. 4 where the binding energies (top) and the two-neutron separation energies (bottom) calculated within SLy4-HFB for Sn isotopes are plotted together with the experimental values (where available). The last bound isotope is ^{176}Sn with this model. To give an idea about the different predictions on the drip line location obtained with different models, we mention that with Gogny D1S-HFB calculations the last bound isotope is ^{160}Sn. Even within the same model, different (and sometimes inappropriate) choices for the pairing interaction may provide a strong model-dependence of the drip line position.

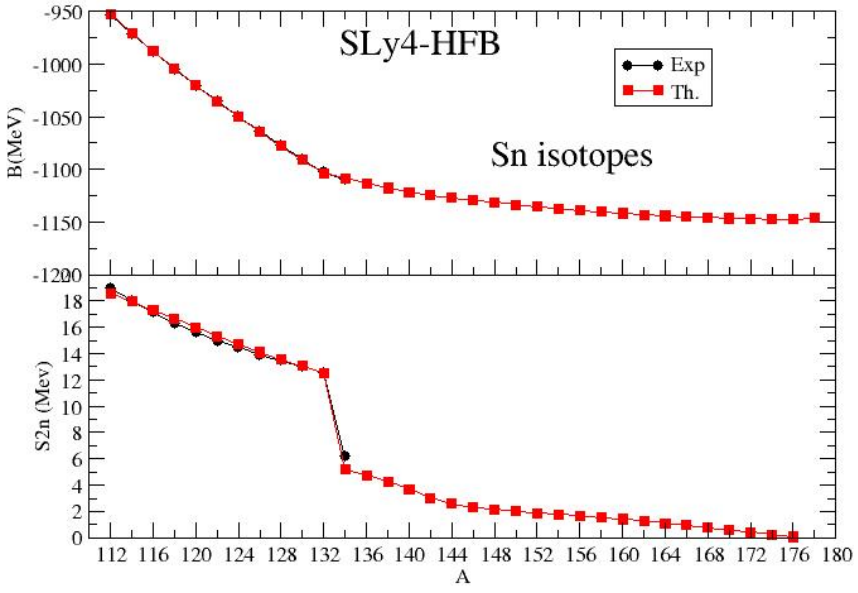

Fig. 4

Binding energies (top) and two-neutron separation energies (bottom) calculated within SLy4-HFB for Sn isotopes. The experimental values are also plotted (where available)

Knowing the ground state structure and wave function, density profiles (and thus radii) and single-particle energies can be evaluated within the mean-field EDF models. Radii of

some magic nuclei are indeed the ingredients (together with the total binding energies) of the fitting procedure of phenomenological interactions.

As far as the single-particle spectrum is concerned, there are two aspects to consider:

1) by construction, the mean-field occupation probabilities are equal to 1 for the hole states which are occupied in the HF state and to 0 for the unoccupied particle states. These occupations are eventually changed around the Fermi energy within the Hartree-Fock-Bogoliubov model if pairing is active in the considered nucleus (but only due to pairing; the other correlations are absent in the HFB model). This means that the mean-field models are not able to describe one important observable which characterizes the single-particle spectra, i.e., the spectroscopic factors. Beyond-mean-field models are necessary to describe the fragmentation of the states and to evaluate the spectroscopic factors.

2) As far as the energies of the single-particle orbitals are concerned, it is worth mentioning that a mean-field evaluation is not a precise prediction of these quantities. The coupling with collective excitations can be important in some cases and the effect of this coupling is a shift of the single-particle energies. The states which are expected to be more affected by this coupling are those located around the Fermi energy, which are in the energy region where the coupling with low-lying excitation modes can become strong. This issue may be crucial in some cases. Let us consider for instance the magicity modifications which have been observed in last years for several exotic nuclei (see, e.g., [Ba07]): some magic numbers desappear, new ones are found and, in general, the gap between the last occupied and the first unoccupied state may evolve along isotopic and isotonic chains of nuclei. Thus, if precise theoretical predictions are required to describe these features, beyond-mean-field models taking into account the particle-vibration coupling have to be employed .

The conclusion we can draw for the above points 1) and 2) is that mean-field models are able to qualitatively predict single-particle spectra but not to make precise and accurate evaluations of their features.

Another aspect related to the single-particle spectra and the shell evolution is the debated question of the tensor contribution. Otsuka first explored this contribution in the framework of the shell model [Ot05] and several analysis have been done later also within the mean-field models with Skyrme and Gogny interactions [Br06, BS07, Co07, Gr07, Le07, Ot06]. In the Skyrme case, the tensor contribution was already present in the first articles of Skyrme of the 50s [Sk56, Sk59]. However, during many years, this contribution has been neglected to simplify the calculations (with some exceptions, for instance, Ref. [SB77]). Apart from the numerical simplification, another reason for neglecting the tensor contribution was that some anomalous behavior had been predicted in Ref. [SB77] when the tensor contribution was included (when the tensor force was included, minor improvements were found in some cases and, in other cases, the agreement with the experimental results was deteriorated).
In the relativistic case, the tensor contribution can be estimated only when the exchange term is included, i.e., in Hartree-Fock or Hartree-Fock-Bogoliubov calculations (and not in Hartree or Hartree-Bogoliubov cases) [Lo06].
An example of the effect of the tensor contribution on single-particle states within the mean-field model is shown in Fig. 5 which is extracted from the work of Colò and collaborators [Co07]. The tensor contribution is included perturbatively on top of the Skyrme interaction Sly5. What is plotted in the figure is the difference of the single-neutron energies $1i_{13/2}$ and $1h_{9/2}$ for the N=82 isotones. This difference is compared with the experimental values of Ref. [Sc04].

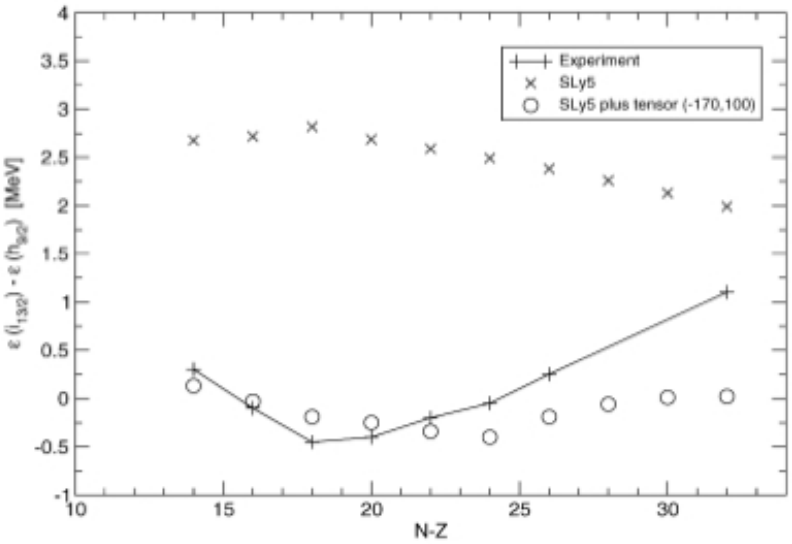

Fig. 5 [Co07]

Energy difference between the $1i_{13/2}$ and $1h_{9/2}$ single-neutron states for the N=82 isotones

VI – DFT AND EDF. DIFFERENCES AND COMMON POINTS

Before starting to enlarge the formal scheme that we are constructing to define the EDF framework, we underline the main differences existing between the two theories EDF and DFT as well as the common points and remind the efforts which are being performed to link the two formalisms:

a) **Both the DFT and the EDF are based on the independent-particle approximation and propose a procedure to simplify the many-body problem by reducing it into a one-body effective problem (however, in the DFT case, correlations are included).**
b) **Both the HF and the KS equations are non-linear and are solved iteratively up to the derivation of the self-consistent solution.**
c) **The ground state is a Slater determinant in both cases.**
d) **In principle, the starting point in the EDF is an interaction (a Hamiltonian in the non-relativistic case) and the functional is derived from the interaction by applying the variational principle. In the DFT, the functional (form and terms) is chosen and not derived from an interaction.**
e) **In nuclear physics, many efforts are devoted to try to use the DFT concepts and procedures: for instance, some attempts to introduce directly the functionals (and not to derive them from an interaction) have been proposed (see, for instance, [Ca08])**
f) **The HK theorems are formulated and demonstrated for a system in an external potential. Nuclei are self-bound and this means that the concepts and theorems of the DFT cannot be exported directly to nuclear physics. Some generalizations are needed in order to formulate them for a self-bound system in the absence of an external potential [En07, Gi-1-08, Gi-2-08, Me09].**
g) **In the HF mean-field equations within EDF, the exchange term is exactly calculated while there is no correlation term. It is however worth mentioning that, even if correlactions are not explicitely introduced, they are in fact included in an effective way in the parameters of the interaction which are fitted to reproduce some observables. In the DFT the exchange term is included, but often in an approximate way, and a correlaction term is always present in the functional.**

h) The concept of symmetry breaking and the related procedures of symmetry restoration are commonly employed in the context of the EDF in nuclear physics. These concepts and procedures are not used in the DFT.
i) When solving the HF and the KS equations, a single-particle spectrum is obtained. However, these energies have a real physical meaning only within the EDF-HF model, not within the DFT-KS approach.
j) A time-dependent formulation of the DFT exists and is based on the Runge-Gross theorem. This means that, in principle, links and extensions between the DFT and the EDF are possible also for all the methods based on time-dependent equations.

VII – PAIRING WITHIN THE MEAN-FIELD MODEL. METHODS AND INTERACTION

The formation of Cooper pairs [BCS57] composed by nucleons is a phenomenon which is well-known in nuclei and confirmed by several experimental observations. This kind of superfluidity manifests itself in many open-shell nuclei. Indeed, even if a conventional interpretation of superfluidity is not really applicable to nuclei because these systems are composed by a relatively small number of constituents, a typical superfluid behavior has been evidentiated by some observations, for instance by moment-of-inertia measurements in rotating deformed nuclei. In the community, the question whether superfluidity in nuclei could be interpreted in an analogous way as superconductivity in electronic systems is debated. Within this interpretation, an important issue for the comprehension of pairing correlations in nuclei would be the description of the exchange of phonons (which in nuclei are the nuclear excited states). For more details about this issue see, e.g., [Ba05].
In the context of the mean field, pairing correlations can be included by a simple extension of the HF model through the introduction of the quasiparticles. When quasiparticles are introduced, the number of particles is not conserved and this symmetry breaking allows one to describe pairing correlations. The derivation of the corresponding HFB or Bogoliubov-de Gennes equations may be found in different books (for example, in Refs. [dG66, RS80]).
We provide here the main points of a derivation inspired by Ref. [dG66]. This derivation is developed for a simplified case: a spherical system, two spin states schematically indicated by $\uparrow$ and $\downarrow$, a central zero-range interaction acting only between opposite spins. If we call V the strength of the interaction and if we suppose that the interaction is well enough described by a two-body term, the Hamiltonian of the system is given by the sum of a one-body term:

$$H_1 = \int d^3\vec{r} \sum_{\alpha} \Psi^+(\vec{r}\alpha) U_1 \Psi(\vec{r}\alpha), \tag{32}$$

and a two-body term:

$$H_2 = \frac{1}{2} V \int d^3\vec{r} \sum_{\alpha\beta} \Psi^+(\vec{r}\alpha)\Psi^+(\vec{r}\beta)\Psi(\vec{r}\beta)\Psi(\vec{r}\alpha), \tag{33}$$

where α and β represent the two spin states and U_1 is the sum of the kinetic term and of an eventual one-body external potential. In the spirit of the mean field, an effective one-body Hamiltonian is introduced:

$$H_{eff} = \int d^3\vec{r}\Big\{\sum_{\alpha} \Psi^+(\vec{r}\alpha)H_e(\vec{r})\Psi(\vec{r}\alpha) + W(\vec{r})\Psi^+(\vec{r}\alpha)\Psi(\vec{r}\alpha) + \Delta(\vec{r})\Psi^+(\vec{r}\uparrow)\Psi^+(\vec{r}\downarrow) + \Delta^*(\vec{r})\Psi(\vec{r}\downarrow)\Psi(\vec{r}\uparrow)\Big\} \tag{34}$$

where H_e is defined by the following relation:

$$H_1 - \lambda N = \sum_{\alpha}\int d^3\vec{r}\Psi^+(\vec{r}\alpha)H_e\Psi(\vec{r}\alpha); \tag{35}$$

N is the operator number of particles,

$$N \equiv \sum_{\alpha}\int d^3\vec{r}\Psi^+(\vec{r}\alpha)\Psi(\vec{r}\alpha), \tag{36}$$

and λ is the chemical potential.
Since H_{eff} is a quadratic form in the operators Ψ and Ψ^+, it can be diagonalized by a unitary transformation such as the Bogoliubov transformations:

$$\begin{aligned}\Psi(\vec{r}\uparrow) &= \sum_n \left(u_n(\vec{r})\gamma_{n\uparrow} - v_n^*(\vec{r})\gamma_{n\downarrow}^+\right),\\ \Psi(\vec{r}\downarrow) &= \sum_n \left(u_n(\vec{r})\gamma_{n\downarrow} + v_n^*(\vec{r})\gamma_{n\uparrow}^+\right).\end{aligned} \tag{37}$$

These transformations define the quasiparticles. They diagonalize H_{eff}, which means:

$$H_{eff} = \varepsilon_0 + \sum_{n\alpha}\varepsilon_n\gamma_{n\alpha}^+\gamma_{n\alpha}\ , \tag{38}$$

where ε_0 and ε_n are the energies of the ground state |0> and of the excited states |n>, respectively. The previous equation may be alternatively written as:

$$\begin{aligned}\left[H_{eff}, \gamma_{n\alpha}\right] &= -\varepsilon_n\gamma_{n\alpha},\\ \left[H_{eff}, \gamma_{n\alpha}^+\right] &= \varepsilon_n\gamma_{n\alpha}^+.\end{aligned} \tag{39}$$

If one calculates [Ψ,H_{eff}] by using eq. (34) and the anticommutation relations for the operators Ψ, one obtains:

$$\begin{aligned}\left[\Psi(\vec{r}\uparrow), H_{eff}\right] &= (H_e + W(\vec{r}))\Psi(\vec{r}\uparrow) + \Delta(\vec{r})\Psi^+(\vec{r}\downarrow),\\ \left[\Psi(\vec{r}\downarrow), H_{eff}\right] &= (H_e + W(\vec{r}))\Psi(\vec{r}\downarrow) - \Delta^*(\vec{r})\Psi^+(\vec{r}\uparrow).\end{aligned} \tag{40}$$

If one uses now the Bogoliubov transformations and eqs. (39), one obtains the HFB equations:

$$\begin{aligned}\varepsilon u(\vec{r}) &= \left[H_e + W(\vec{r})\right]u(\vec{r}) + \Delta(\vec{r})v(\vec{r}),\\ \varepsilon v(\vec{r}) &= -\left[H^*_e + W(\vec{r})\right]v(\vec{r}) + \Delta^*(\vec{r})u(\vec{r}).\end{aligned} \tag{41}$$

In the above equations, W and Δ are the mean field and the pairing field, respectively. They may be derived by applying the variational principle. One imposes that the free energy is stationary:

$$0 = \delta F = \delta\langle H\rangle - T\delta S, \tag{42}$$

where the mean value of H is defined as:

$$\langle H\rangle \equiv \frac{\sum_\phi \langle\phi|H|\phi\rangle \exp\left(-\beta E_\phi\right)}{\sum_\phi \exp\left(-\beta E_\phi\right)}, \qquad \beta = \frac{1}{K_B T}. \tag{43}$$

By evaluating $\langle H\rangle=\langle H_1+H_2\rangle$ with the Wick theorem, one can write an expression for δF. Then, if one supposes that also $F_1=\langle H_{eff}\rangle - TS$ (calculated with the states which diagonalize H_{eff}) is stationary, an expression for δF_1 can be obtained. By comparing it with the expression of δF, one concludes that F is stationary if:

$$\begin{aligned} W(\vec{r}) &= V\left\langle \Psi^+(\vec{r}\uparrow)\Psi(\vec{r}\uparrow)\right\rangle = V\left\langle \Psi^+(\vec{r}\downarrow)\Psi(\vec{r}\downarrow)\right\rangle, \\ \Delta(\vec{r}) &= V\left\langle \Psi(\vec{r}\downarrow)\Psi(\vec{r}\uparrow)\right\rangle = -V\left\langle \Psi(\vec{r}\uparrow)\Psi(\vec{r}\downarrow)\right\rangle. \end{aligned} \tag{44}$$

One can thus define the particle and the pairing or anomalous densities :

$$\rho(\vec{r}) \equiv \left\langle \Psi^+(\vec{r}\alpha)\Psi(r\alpha)\right\rangle = \sum_n \left[(1-f_n)v_n^2(\vec{r}) + f_n u_n^2(\vec{r})\right], \tag{45}$$

$$\tilde{\rho}(\vec{r}) \equiv \left\langle \Psi(\vec{r}\downarrow)\Psi(r\uparrow)\right\rangle = -\sum_n \left[(1-2f_n)v_n^*(\vec{r})u_n(\vec{r})\right], \tag{46}$$

where f_n is a Fermi function providing the temperature-dependence:

$$f_n = \frac{1}{\exp(\beta\varepsilon_n)+1}. \tag{47}$$

In the nuclear case, these equations are usually used in the simpler case of zero temperature. However, the expressions for the interaction are much more complicated than the one used in this simple derivation (see Sec. IV) leading to more complicated expressions for the potentials.
If one imposes that the pairing field couples only time-reversed states, a simplification of the HFB equations is obtained corresponding to a simplified form of the Bogoliubov transformations and leading to the model of Bardeen, Cooper and Schrieffer which has been introduced in the 50s to describe Cooper pairs of electrons in superconductors [BCS57]. In nuclear physics, this approximation of the HFB model is called HF+BCS.

When dealing with the HFB equations, a very important concern is the choice of the interaction to be used in the pairing channel of the equations. In the non-relativistic case, one distinguishes between the mean-field models with the Gogny and with the Skyrme interactions.
For the Gogny case, the same interaction is introduced and fitted to be used in both the mean-field and the pairing channels. For the Skyrme case, the parameters of the interaction are usually fitted only at the Hartree-Fock level (with the exception of the

parametrization SkP [Do84]). A different interaction has thus to be introduced in the pairing channel of the equations and several strategies may be followed.
We distinguish between fundamental and phenomenological procedures to construct these functionals and provide some examples. Among the more fundamental procedures, we mention the derivation of a non-empirical pairing functional obtained at lowest order in many-body perturbation theory [He09]. By assuming the validity of the LDA, another procedure as been recently proposed where the interaction is derived from a microscopic nucleon-nucleon interaction and a fit to reproduce the pairing gap in symmetric and neutron matter is performed [Ma08]. In this case, the form of the pairing interaction has been enriched (with respect to the usual zero-range density-dependent interaction) and a linear dependence on the isovector density has been added.
When empirical pairing functionals are used, the starting point is a phenomeological interaction and its parameters are fitted to reproduce some observables. The interaction which is currently used has a zero-range and depends on the isoscalar density:

$$V_{pair} = V_0 \left[1 - \eta \left(\frac{\rho(r)}{\rho_0} \right)^{\alpha} \right] \delta\left(\vec{r}_1 - \vec{r}_2 \right); \qquad \textbf{(48)}$$

ρ_0 is commonly chosen equal to the saturation density. The parameters V_0, η and α are usually fitted by using constraints such as the odd-even mass staggering and/or the separation energies. It is worth mentioning that also in the case of phenomenological interactions some attempts to enrich the interaction with a dependence on the isovector density (linear and quadratic) have been proposed [Ya09].
Beyond the question of enriching and improving the form of the interaction, another issue is discussed, namely whether the fitting procedure should be eventually modified by introducing different constraints. For instance, there are some theoretical indications suggesting that experimental measurements of pairing vibrations (with two-nucleon transfer reactions) may guide towards a deeper comprehension of the pairing interaction. QRPA calculations with different pairing interactions (a different volume-surface mixing obtained by modifying the parameter η in eq. (48)) provide different response functions and transition densties [Gr09, Kh09, Ma09].
It is important noticing that the zero-range of the pairing interaction leads to a well known ultraviolet divergence in the pairing channel that is usually treated by choosing a numerical energy cutoff and by considering it as a parameter in the fitting procedure. A regularization method of the ultraviolet divergence is currently used in atomic physics [Br99, Gr03] and has been proposed for the nuclear case by Bulgac and Yu [Bu02]. It is based on the concept of pseudopotential [Hu87]. In Fig. 6 the neutron pairing field profile is plotted for different cutoff energies E_C. Upward various curves correspond to E_c = 20, 30, 35, 40, 45 and 50 MeV, respectively. The last two curves are indistinguishable showing that the ultraviolet divergence has been regularized. The figure is extracted from Ref. [Bu02].

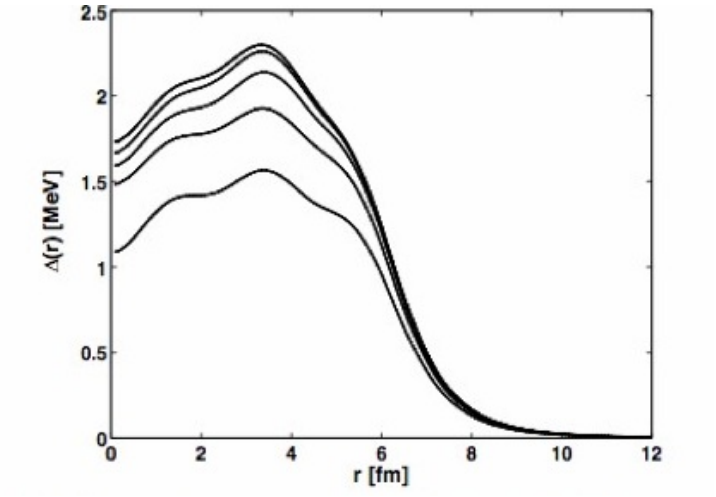

Fig. 6 [Bu02]

The neutron pairing field profiles are plotted for different cutoff energies E_C. Upward various curves correspond to E_C = 20, 30, 35, 40, 45 and 50 MeV, respectively.

VIII – SMALL-AMPLITUDE EXCITATIONS FROM THE TIME-DEPENDENT MEAN-FIELD METHODS: (Q)RPA

Time-dependent mean-field methods are suitable to treat the dynamical evolution of a system in the mean field approximation (see, for instance, Refs. [AS08, AW09, GS09, SAL07]).
The TDHF and TDHFB equations are given by the following expressions:

$$i\hbar \frac{d\rho}{dt} = \left[h + f(t), \rho\right], \tag{49}$$

$$i\hbar \frac{d\Re}{dt} = \left[\bar{h} + f(t), \Re\right], \tag{50}$$

respectively, where f(t) is an external perturbation; ρ and h in eq. (49) are the density and the HF Hamiltonian, respectively. $\Re$ and $\bar{h}$ in eq. (50) are the generalized density (containing also the pairing tensor [Kh02]) and the HFB Hamiltonian, respectively.

An example of applications of time-dependent approaches is given in Fig. 7 [GS09]. The TDHF theory is used there to study the collision dynamics of two ^{238}U nuclei.

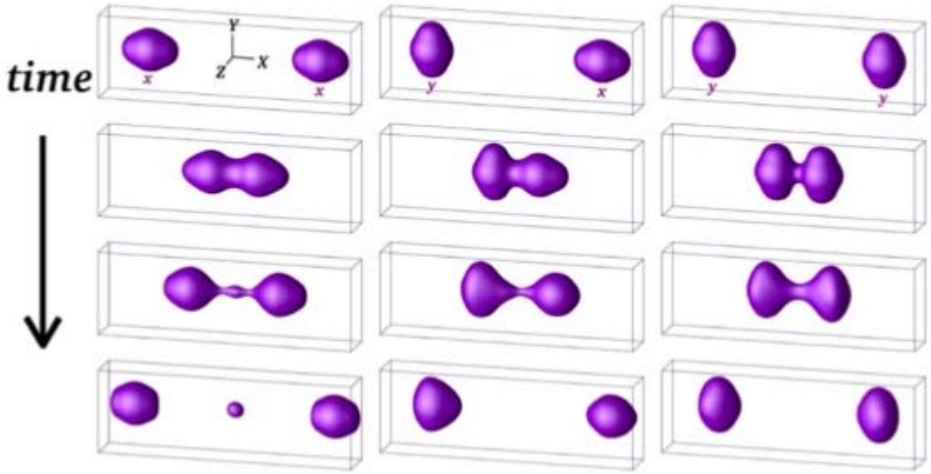

Fig. 7 [GS09]

^{238}U + ^{238}U central collision. Evolutions associated to 3 different initial configurations. See [GS09] for details

In the limit of a weak perturbing field the linear response theory can be applied, i.e., the response of the system can be approximated by a linear variation with respect to the external field. In the limit of a weak perturbing field, within the linear response theory, the perturbed density performs small-amplitude oscillations. From the small-amplitude limit of the TDHF(B) model, the (Q)RPA equations may be derived (see [Kh02, RS80] for details). In this formal derivation use is made of the quasiboson approximation (QBA) [RS80]. The nature of this approximation is easier to understand in a different framework, where the RPA equations are obtained within the equations-of-motion method [Ro68, RS80].
The RPA ground state is defined as the vacuum of the operators Q_υ:

$$Q_\nu \left| \mathrm{RPA} \right\rangle = 0 \,, \tag{51}$$

where the operators Q_ν^+ are defined as superpositions of particle-hole and hole-particle configurations:

$$Q_\nu^+ \equiv \sum_{ph} \left(X_\nu^{ph} a_p^+ a_h - Y_\nu^{ph} a_h^+ a_p \right). \tag{52}$$

We use the conventional notation : p and h stand for the quantum numbers of particle and hole states (with respect to the HF ground state). The operators Q_ν^+ create the RPA phonons by acting on the RPA ground state:

$$Q_\nu^+ \left| \mathrm{RPA} \right\rangle = \left| \nu \right\rangle . \tag{53}$$

The presence of the term depending on the amplitudes Y in the expression for the operators Q_ν^+ (eq. (52)) means that the RPA ground state is in principle correlated and different from the HF ground state.
Using the equations-of-motion method (starting from the stationary Schrödinger equation) the RPA equations may be derived:

$$\begin{pmatrix} A & B \\ B^* & A^* \end{pmatrix}\begin{pmatrix} X^\nu \\ Y^\nu \end{pmatrix} = (E_\nu - E_0)\begin{pmatrix} 1 & 0 \\ 0 & -1 \end{pmatrix}\begin{pmatrix} X^\nu \\ Y^\nu \end{pmatrix}. \tag{54}$$

The matrices A and B are defined as:

$$\begin{aligned} A_{ph,p'h'} &\equiv \langle RPA | \left[a_h^+ a_p, H, a_{p'}^+ a_{h'} \right] | RPA \rangle, \\ B_{ph,p'h'} &\equiv -\langle RPA | \left[a_h^+ a_p, H, a_{h'}^+ a_{p'} \right] | RPA \rangle, \end{aligned} \tag{55}$$

where H is the Hamiltonian of the system and

$$[A,B,C] \equiv \frac{1}{2}([A,[B,C]] + [[A,B],C]). \tag{56}$$

When the interaction is density-dependent, it can be shown that:

$$A_{ph,p'h'} = (\varepsilon_p - \varepsilon_h)\delta_{pp'}\delta_{hh'} + \frac{\partial h_{ph}}{\partial \rho_{p'h'}}, \tag{57}$$

$$B_{ph,p'h'} = \frac{\partial h_{ph}}{\partial \rho_{h'p'}}. \tag{58}$$

Since h (the HF Hamiltonian) is the derivative with respect to the density of the Hamiltonian density (the energy density functional), the RPA residual interaction in the above two expressions is the second derivative with respect to the density of the energy density functional. It means that the residual interaction contains rearrangement terms coming from the density-dependence of the interaction.
The solutions of Eqs. (54) are the energies and the wave functions (X and Y amplitudes) of the excited states. To simplify the problem, the QBA approximation is employed in the evaluation of the matrices A and B. This approximation can be written as:

$$\begin{aligned} &\left\langle RPA \left| \left[a_h^+ a_p, a_{p'}^+ a_{h'} \right] \right| RPA \right\rangle \\ &= \delta_{hh'}\delta_{pp'} - \delta_{pp'}\left\langle RPA \left| a_{h'} a_h^+ \right| RPA \right\rangle - \delta_{hh'}\left\langle RPA \left| a_{p'}^+ a_p \right| RPA \right\rangle. \\ &\approx \left\langle HF \left| \left[a_h^+ a_p, a_{p'}^+ a_{h'} \right] \right| HF \right\rangle = \delta_{pp'}\delta_{hh'} \end{aligned} \tag{59}$$

The use of the QBA generates two problems related one to the other:
(i) the Pauli principle is violated because some terms are neglected in Eq. (59). The final expression would be correct if the pair of operators 'a^+a' was a bosonic operator (from this feature derives the name of the approximation);

(ii) in principle, the RPA ground state should contain some correlations but, in practice, it is replaced by the uncorrelated HF ground state. The Pauli principle violation is thus related to the use of the HF state instead of the RPA state. Hence, the violation is more important if the ground state is actually strongly correlated.

Some solutions to overcome these problems are mentioned in Sec. X.A.

The QRPA method is a generalization of the RPA model where pairing correlations are added through the introduction of the quasiparticles. The reference ground state is the HFB state instead of the HF state. As an illustration of QRPA applications we show in Fig. 8 the isoscalar quadrupole strength function calculated for the nucleus ^{22}O (solid line). The unperturbed strength is also shown (dotted line). The figure is taken from Ref. [Kh02].

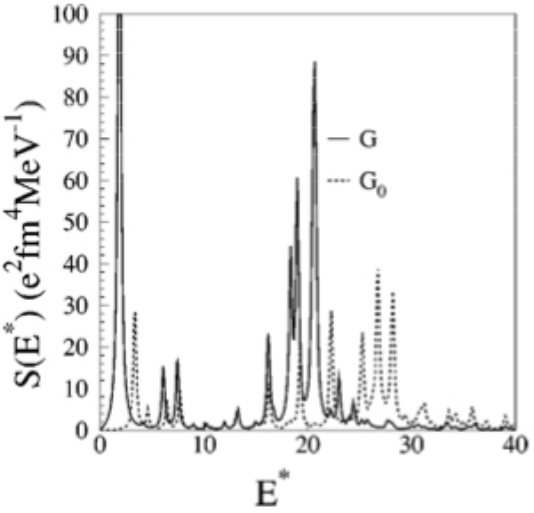

Fig. 8 [Kh02]

QRPA isoscalar quadrupole strength function calculated for the nucleus ^{22}O (solid line). The unperturbed strength is also shown (dotted line)

IX – BEYOND MEAN-FIELD MODELS - I. COUPLING OF INDIVIDUAL AND COLLECTIVE DEGREES OF FREEDOM

In a mean-field analysis of the ground state single-particle features are the relevant degrees of freedom which are explicitely taken into account: in the context of the HF model, the ground state is a pure Slater determinant, i.e., an uncorrelated state given by an antisymmetrized product of single-particle wave functions. On the other hand, the RPA allows one to treat collective degrees of freedom in order to describe the excited states.
In nuclei and, in general, in all many-body systems collective and individual degrees of freedom coexist and may couple; a more complete treatment of nuclear properties should thus go beyond the simple HF and RPA schemes and should include this coupling (particle-vibration or particle-phonon coupling).
The increasing interest and the efforts devoted to go beyond-mean-field in this direction are also justified by the manifestation of new phenomena in the excitation spectra of some neutron-rich nuclei. For instance, pygmy resonances represent exotic low-lying excitation modes related to the presence of a neutron skin in neutron-rich nuclei. The necessity to go beyond standard-mean-field models to describe these resonances has been demonstrated by the important effects found when the particle-vibration coupling is included (see, for instance, Ref. [Te07]). More in general, several low-lying excited states may be affected by the particle-phonon coupling. This coupling provides a shift of the excitation energies as well as a fragmentation of the excited states which allows one to partially describe the spreading widths of the excitation modes (see Ref. [Be83] for a review about the widthts of the excited states).
In the SRPA model, the inclusion of the 2 particle-2 hole configurations also allows a partial description of the widths.

Due to this common point between the two approaches (the particle-vibration coupling and the SRPA), they are presented here in the same section.

IX.A - Particle-vibration coupling

In a particle-vibration coupling description, one should in principle couple the single-particle degrees of freedom with both particle-hole and particle-particle excitations. However, it has been demonstrated by Bertsch and collaborators that the particle-particle vibrations contribute much less to the modification of the single-particle states [Be79]. The particle-vibration coupling, described by taking into account only particle-hole excitations (calculated with the RPA model), modifies the HF mass operator in the following way [Be80, Br05, Co01, Li07]:

$$M(E) = M^{HF} + \Sigma(E), \tag{60}$$

where:

$$\Sigma(E) = \Sigma^{RPA}(E) - \Sigma^{(2)}(E). \tag{61}$$

The correction Σ^{RPA} in Eq. (61) is described by the following two diagrams:

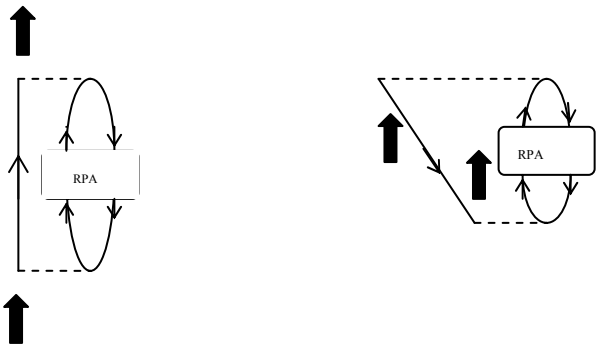

The diagram on the left is called polarization graph and that on the right is called correlation diagram. The second-order diagrams

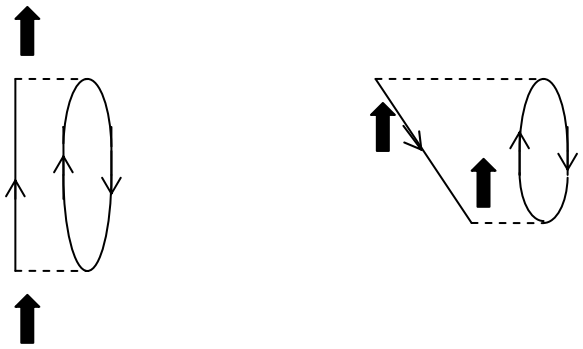

have to be substracted to correct for the double counting introduced because the RPA phonons are used to treat the particle-phonon coupling [Be80].
The particle-vibration coupling generates a shift of the individual energies (and also of the energies of the excited low-lying modes) and a fragmentation of the single-particle states (as well as of the excited modes). The fragmentation of the excitation modes allows one to partially describe their width while that of the single-particle states provides a description of the spectroscopic factors.

Effective masses are generated by the non-locality and the energy-dependence of the nuclear potential. The non-locality provides the k-mass $\tilde{m}$:

$$\frac{\tilde{m}}{m} = \left(1 - \frac{m}{\hbar^2 k}\frac{\partial M}{\partial k}\right)^{-1}, \qquad (62)$$

where M is the mass operator. The energy-dependence generates the E-mass $\overline{m}$:

$$\frac{\overline{m}}{m} = 1 - \frac{\partial M}{\partial E}. \qquad (63)$$

The effective mass m* is defined as:

$$\frac{m^*}{m} = \frac{\tilde{m}}{m} \times \frac{\overline{m}}{m}. \qquad (64)$$

It turns out that $\overline{m}/m$ is the inverse of the spectroscopic factor S_α for a given state α: $S_\alpha \leq 1$ means that $\overline{m}/m \geq 1$. Thus: $m^* \geq \tilde{m}$.
In the HF model $\overline{m}/m = 1$ because the potential does not depend on the energy and $m^* = \tilde{m}$. When the particle-vibration coupling correction is added to the HF mass operator, an energy-dependence is included and the E-mass becomes larger than 1. The spectroscopic factors S_α may thus be evaluated.

If the Skyrme interaction is used to describe the particle-vibration coupling an ultraviolet divergence occurs related to the zero-range of the interaction. The energy cutoff is thus a very delicate and important parameter in this kind of calculations.

Two examples of the particle-vibration effect are shown in Figs. 9 and 10.
Fig. 9 is extracted from Ref. [Be80] and shows the shift of the single-neutron energies in ^{208}Pb associated to the particle-vibration coupling (E_α in the figure).
Fig. 10 shows the effect on the excited states. The figure is taken from Ref. [Li07]. The isovector E1 resonance is calculated with different models (see [Li07] for details) for ^{208}Pb (left) and ^{132}Sn (right). The results where the particle-vibration coupling is included are displayed by solid lines.

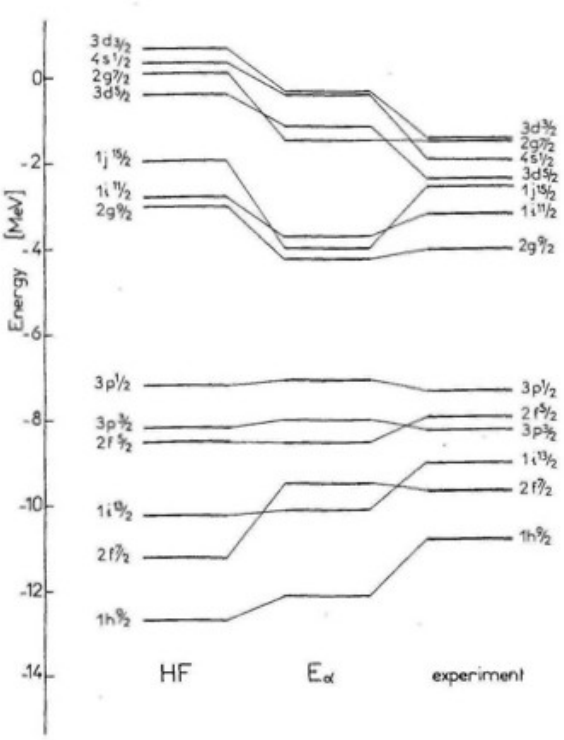

Fig. 9 [Be80]

Neutron single-particle states for ^{208}Pb. Left: HF; middle: HF + particle-vibration coupling; right: experimental values

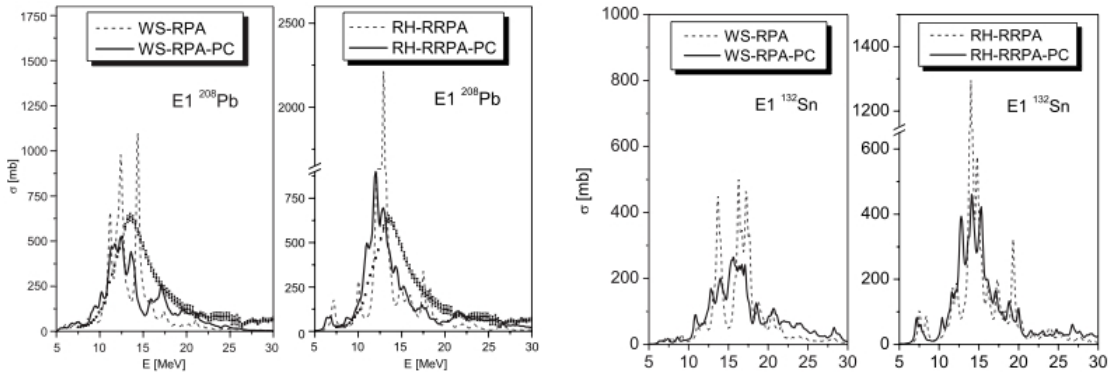

Fig. 10 [Li07]

The isovector E1 resonance is calculated with different models (see [Li07] for details) for ^{208}Pb (left) and ^{132}Sn (right).

IX.B - SRPA

The RPA is currently used to describe the excitation spectrum of a quantum many-body system. Its success in nuclear physics is well established and the method has been applied for many years to describe giant resonances and low-lying excitation modes.
A natural extension of the RPA, also based on the approximation QBA, is the SRPA method where 2 particle-2 hole (2p2h) excitations are included together with the usual RPA 1

particle-1 hole (1p1h) configurations providing in this way a richer description of the excitation modes (for both the energies and the widths).
The SRPA equations have been derived by following different procedures. Some examples are the derivation within the equations-of-motion method [Ya-1-86], the procedure employing a variational approach [Pr65] or the small-amplitude limit of the time-dependent density matrix (TDDM) [La04, To89]. However, up to very recently, the SRPA equations have never been fully and self-consistently solved because of the heavy numerical effort which they require. Some approximations have been adopted in the past, namely the SRPA equations have been reduced to a simpler second Tamm-Dancoff model (i.e., the matrix B is put equal to zero; see, for instance, Refs. [Ho76, Kn76, Ni95, Ni98]) and/or the equations have been solved with uncorrelated 2p2h states: the residual interaction terms in the matrix that couples 2p2h configurations among themselves have been neglected (diagonal approximation) [Ad78, Dr-1-86, Dr-2-86, Sc-1-84, Sc-2-84, Ya83, Ya-2-86].
Very recently, this problem has regained a new interest; it is becoming now numerically more accessible and the SRPA equations have been solved for closed-shell nuclei using an interaction derived from the Argonne V18 potential (with the Unitary Correlation Operator Method) [Pa-1-09, Pa-2-09], for small metallic clusters in the jellium approximation [Ga09] and for the nucleus ^{16}O with the Skyrme interaction [Ga10].
We briefly recall the main formal aspects of the SRPA model which may be found in several articles (see, for instance, Ref. [Ya-1-86}). The equations are a natural extension of the RPA problem where the excitation operators Q^{+}_{υ} are a superposition of 1p1h and 2p2h configurations:

$$Q^{+}_{\nu} = \sum_{ph}\left(X^{\nu}_{ph}a^{+}_{p}a_{h} - Y^{\nu}_{ph}a^{+}_{h}a_{p}\right) + \sum_{p<p',h<h'}\left(X^{\nu}_{php'h'}a^{+}_{p}a_{h}a^{+}_{p'}a_{h'} - Y^{\nu}_{php'h'}a^{+}_{h}a_{p}a^{+}_{h'}a_{p'}\right). \quad (65)$$

The X's and Y's are solutions of the equations

$$\begin{pmatrix} A & B \\ -B^{*} & -A^{*} \end{pmatrix}\begin{pmatrix} X^{\nu} \\ Y^{\nu} \end{pmatrix} = \omega_{\nu}\begin{pmatrix} X^{\nu} \\ Y^{\nu} \end{pmatrix}, \quad (66)$$

where:

$$A = \begin{pmatrix} A_{11} & A_{12} \\ A_{21} & A_{22} \end{pmatrix}; \quad B = \begin{pmatrix} B_{11} & B_{12} \\ B_{21} & B_{22} \end{pmatrix}; \quad (67)$$

$$X^{\nu} = \begin{pmatrix} X^{\nu}_{1} \\ X^{\nu}_{2} \end{pmatrix}; \quad Y^{\nu} = \begin{pmatrix} Y^{\nu}_{1} \\ Y^{\nu}_{2} \end{pmatrix}, \quad (68)$$

and the indices 1 and 2 are a short-hand notation for the 1p1h and 2p2h configurations, respectively.
In Eq. (67), A_{11} and B_{11} are the usual RPA matrices, A_{12} and B_{12} are the matrices coupling 1p1h with 2p2h configurations and A_{22} and B_{22} are the matrices coupling 2p2h configurations among theselves. If the QBA is used and the HF ground state is thus employed to evaluate these matrix elements, it can be shown that B_{12} and B_{22} are zero. The expressions for the other matrix elements may be found, for instance, in Ref. [Ya-1-86]. These expressions are valid in the case where the interaction is not density-dependent. Rearrangement terms should be included in the case of density-dependent forces.

Some comments about the use of the QBA in the SRPA model can be found in the literature [Ga06, La90]: it is said that the use of the QBA in the SRPA is a more drastic and severe approximation than in RPA. This can be easily understood within the variational derivation of the SRPA provided by Providencia [Pr65].
The usual way of writing the RPA ground state is

$$|\Psi\rangle = e^{\hat{S}}|\Phi\rangle, \tag{69}$$

where:

$$\hat{S} = \sum_{ph} C_{ph}(t) a_p^+ a_h \,, \tag{70}$$

the operator $\hat{S}$ being a superposition of 1p1h configurations built on top of HF ground state $|\Phi\rangle$. The expression of the SRPA ground state in Ref. [Pr65] is the same as Eq. (69) where now the operator $\hat{S}$ also contains 2p2h terms:

$$\hat{S} = \sum_{ph} C_{ph}(t) a_p^+ a_h + \frac{1}{2} \sum_{php'h'} C_{pp'hh'}(t) a_p^+ a_{p'}^+ a_h a_{h'} \,. \tag{71}$$

This means that the ground state is no longer a Slater determinant. Due to this, the use of the HF ground state to calculate the matrix elements (QBA) is a stronger approximation than in RPA. Extensions to cure this problem in the context of SRPA have been proposed and applied to a simple model [Ga06] and to metal cluster [Ga09]. Future applications to nuclei are in progress.
We show now in Fig. 11 one example of SRPA strength distributions obtained for the nuclei ^{48}Ca and ^{16}O. We refer to the papers [Pa-1-09, Pa-2-09] for the details of the calculations. One observes that the strongest effect in SRPA is a several-MeV shift of the strength distribution to lower energies with respect to RPA. This result seems to be a general feature of the SRPA and has been found also in SRPA calculations performed for metallic clusters [Ga09].

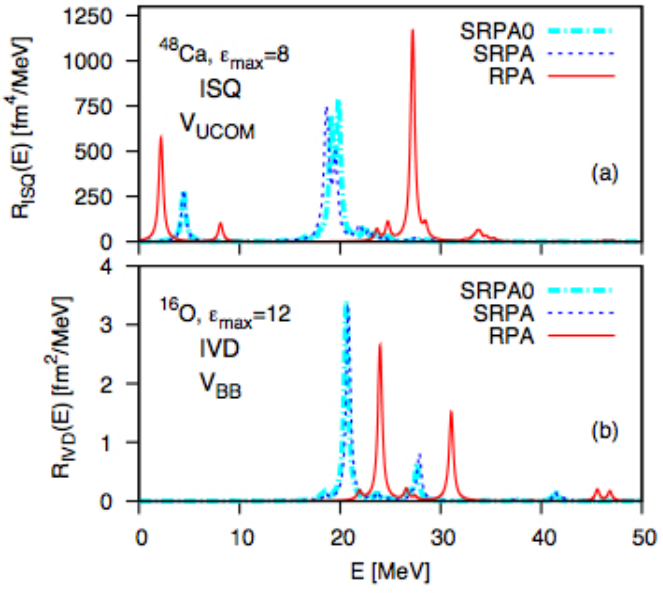

Fig. 11 [Pa-2-09]

Top: isoscalar quadrupole response for ^{48}Ca. Bottom: isovector dipole response for ^{16}O

X – BEYOND MEAN-FIELD MODELS - II. A CORRELATED GROUND STATE

In order to go beyond standard mean-field based approaches, two directions (among several others) may be explored: i) coupling single-particle and collective degrees of freedom; ii) introducing in an explicit way correlations in the ground state. The first issue has been discussed in the previous section. This section is devoted to the second issue.
It has been stated above that the RPA ground state is supposed to be correlated; in practice, however, the QBA approximation (see Section VIII) is employed in the standard RPA corresponding to the use of the uncorrelated HF ground state in the evaluation of the matrix elements. As it has been previously underlined, this leads to a lack of consistency in the model as well as to a violation of the Pauli principle.
Several extensions and procedures to go beyond and improve the treatment of the correlations have been introduced in the past decades.

X.A – EXTENSIONS OF RPA AND SRPA

A possible way to explicitely introduce correlations in the ground state consists in costructing an RPA-like formalism where the violations of the Pauli principle related to the use of the QBA are cured. Two main lines have been developed in the past decades using either boson expansion methods [Be92, Ca89, Ga-1-06, Gr02, Sa95, Sa97, Sa99, Vo99] or extensions in the fermionic space [Ca98, Du90, Du96, Ga06, Ka93, Kl91, Kr98, Ra98, Ta04, To07]. Many of these approaches are based on the so-called renormalized RPA (RRPA) method starting from the hearly works of Hara and Rowe in the 60s (see Ref. [Ha64]). In all these RRPA models: (i) the ground state is explicitely correlated with occupation numbers different from 1 and 0 appearing in some renormalization factors; (ii) the Pauli principle is satisfied because the QBA is not adopted. However, all the models based on a RRPA are strongly limited by the fact the the Energy Weighted Sum Rules (EWSRs)

$$\sum_{\nu} \left(E_{\nu} - E_0\right) \left|\langle \nu | F | 0 \rangle\right|^2 = \frac{1}{2} \langle 0 | [F, [H, F]] | 0 \rangle \qquad (72)$$

are not satisfied, where F is a 1-body hermitian operator. Some possible lines to overcome this drawback have been proposed in Refs. [Ga-1-09, Gr00].

X.B – GCM AND MULTIPARTICLE-MULTIHOLE CONFIGURATION INTERACTION METHOD

In both the GCM and the multiparticle-multihole configuration interaction method a correlated ground state is explicitely considered (superposition of mean-field states).

The GCM is a variational method which extends the configuration mixing to the case of a continuous collective variable. It turns out that all the projection methods which are used to restore broken symmetries are special forms of the GCM. For a detailed introduction of the formalism of the GCM, Ref. [Bo90] is recommended.
The wave functions are expressed as linear combinations of a family of wave functions depending on some collective variables. For this particular feature, the GCM is suitable to describe collective phenomena and large amplitude deformations. Given a family of N-

body wave functions $|\Phi(q)\rangle$ depending on a collective variable q, the GCM determines approximate states of the Hamiltonian of the form:

$$\left|\Psi_k\right\rangle = \int dq f_k(q) \left|\Phi(q)\right\rangle . \qquad (73)$$

The coefficients f_k are found by imposing that

$$E_k = \frac{\left\langle \Psi_k \left| H \right| \Psi_k \right\rangle}{\left\langle \Psi_k \left| \Psi_k \right. \right\rangle} \qquad (74)$$

is stationary with respect to the variations δf_k.
The coupling between collective and single-particle degrees of freedom is implicitely taken into account in the GCM (in the use of the deformed mean field). However, only collective degrees of freedom have been considered so far as generating coordinates (quadrupole, octupole, pairing,...). Some efforts are devoted to try to use indices of quasiparticles as generator coordinates; in this way, an explicit coupling between single-particle and collective coordinates would be introduced.
For many applications, the most important generator coordinate is the quadrupole deformation, but other degrees of freedom have been considered as well [Be-1-08, Eg04].
Nowadays, GCM-type configuration mixing is almost always combined with projection on particle number and angular momentum. Such approach gives a correlated ground state and a spectrum of excited states for each angular momentum, and allows for the calculation of transition moments that respect selection rules. There exist implementations using Skyrme and Gogny interactions, as well as relativistic Lagrangians. Typical results can be found in Refs. [Be-2-08, Be04, Ni-1-06, Ni-2-06, Ro02, Ro05].
Exact symmetry-restored GCM is numerically heavy, in particular when several generator coordinates are considered simultaneously (recent applications [Be-2-08,Ro10] consider 7 generator coordinates: the 5 components of the quadrupole tensor and two gauge angles that correspond to particle-number projection). It can be used, however, as the starting point to derive a microscopic Bohr Hamiltonian (see [Kl08, Li99, Ni09] and references therein) that is numerically much simpler to handle and that allows easily to add higher-order corrections to the moments of inertia.
Both the symmetry-restored GCM [Be-3-08] and the mapped collective Hamiltonian [De10] have been used for large-scale investigations of ground-state correlations and properties of characteristic excited states.
It has to be mentioned that some technical problems (jumps and divergences) have been found in applications of the GCM [An01, Do07] that employ an energy functional that cannot be mapped onto an underlying effective interaction (by contrast, a GCM based on a non-density dependent Hamilton operator is not subject to these difficulties). A regularization scheme to solve these problems has been proposed and applied in Refs. [Be-1-09, Du09, La09].

In a multiparticle-multihole configuration mixing approach, the correlations are included by considering a ground state given by a superposition of Slater determinants. A Higher Tamm Dancoff approximation [Bo07, Qu04, Si07] and a variational multiparticle-multihole configuration mixing approach [Pi08] have been proposed in the literature. It should be mentioned that in the Higher Tamm Dancoff case the model is not developed in the framework of the EDF (the residual interaction is not derived from the energy density functional).
In Ref. [Pi08], the wave function of the system is chosen as a superposition of a finite set of Slater determinants which includes the HF state and multiple particle-hole excitations of this state. Both the configuration-mixing coefficients and the single-particle states are found with a variational procedure. This formal scheme is developed in the framework of

the EDF. The Gogny interaction is used to construct the energy density functional and the residual interaction is derived from the Gogny interaction.

XI – NUCLEAR ASTROPHYSICS. NEUTRON STARS. SOME APPLICATIONS OF THE EDF MODELS

Neutron stars, the most compact stellar objects after black holes, are the remnants of core collapse supernovae [Be90, Gl97]. A detailed description of the structure and the properties of neutron stars can be found in the Lectures of P. Pizzochero.
The physics of neutron stars is a multidisciplinary domain where nuclear physics plays a very important role. The description of those neutron-star properties which are not directly linked to the observations such as, for instance, their internal composition, requires the development of theoretical models where the ingredients coming from nuclear physics are very important. Furthermore, the comprehension of several properties of neutron stars may be obtained from the study of the properties of atomic nuclei. In a natural way, the link between neutron stars and nuclei is made via the nuclear matter: it turns out that asymmetric nuclear matter is rather similar to the matter found in neutron stars which is called neutron-star matter. Recently, more direct relations between neutron-rich nuclei and neutron-star matter have been proposed.

Isospin asymmetry is a common feature characterizing both neutron-rich nuclei and neutron stars; this asymmetry can be ~ 0.95 in the interior of the star. The dependence of several properties of nuclear systems on the isospin asymmetry may be related to the symmetry energy, E_{sym}, defined by an expansion of the energy with respect to the asymmetry $\delta=(\rho_n-\rho_p)/\rho$,

$$E(\rho, \delta) \sim E_0(\rho) + E_{sym}(\rho)\,\delta^2 + \ldots,$$

where ρ is the total density and ρ_n and ρ_p are the neutron and proton densities, respectively.
It turns out that the pressure of neutron matter (which is not so different from neutron-star matter) is related to $\rho^2 \partial E_{sym}/\partial\rho$. The density-dependence of the symmetry energy is thus very important in determining all the properties associated to the pressure. Due to this feature, some relations between neutron-rich nuclei and neutron-star properties have been found. To mention some examples: (a) Lattimer and Prakash found the existence of correlations between the neutron star radius and the pressure evaluated at densities above the equilibrium density [LP00, LP01]; (b) Typel and Brown pointed out the existence of correlations between the neutron skin thickness in nuclei and the pressure of neutron matter evaluated at sub-nuclear densities [Br00, TB01]; (c) Horowitz and Piekarewicz found a relation between the neutron skin thickness in nuclei and the neutron star radius [HP01].
What is shown in Fig. 12 is the calculated neutron skin thickness δR of nuclei as a function of the radius of stars of mass equal to 1.4 solar masses (left panel) and as a function of the radius of maximum-mass stars (right panel). The figure is extracted from the work of Steiner and collaborators [St05]. Symbols represent results of EDF model calculations and provide thus a first example of applications of EDF models to astrophysical issues, namely the description of neutron star properties (see [St05] for details about the shown results).

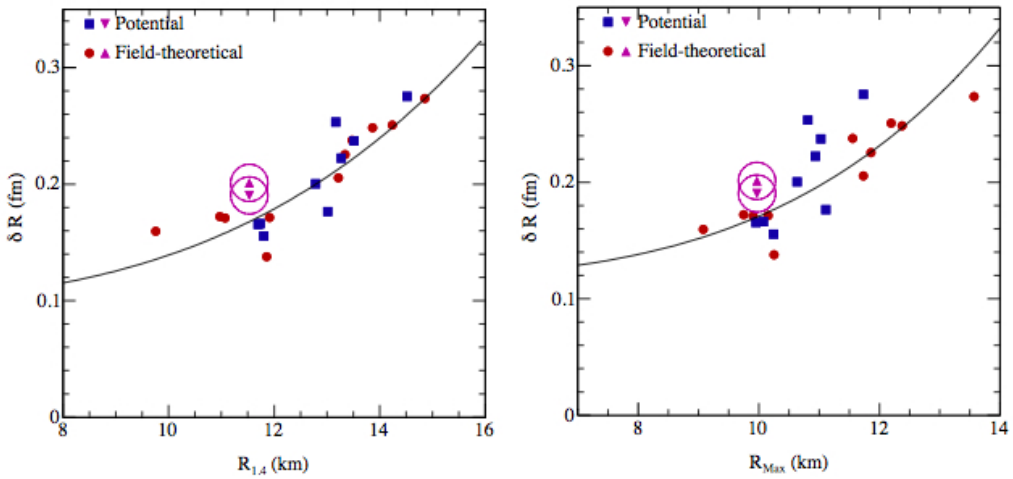

Fig. 12 [St05]

Calculated neutron skin thickness of nuclei versus the radius of stars of mass equal to 1.4 solar masses (left panel) and versus the radius of maximum-mass stars (right panel)

Another very direct link exists between nuclei and neutron stars: some exotic neutron-rich nuclei produced in nuclear facilities are actually also located in the outer crust of neutron stars surrounded by electrons (while the inner crust is composed by beyond-drip-line nuclear systems surrounded by a neutron gas and by electrons). Thus, the comprehension of the properties of these nuclei (for instance, the description of pairing correlations) has a direct impact on the comprehension of neutron star properties.

Neutron stars evolve with time and new phenomena occur. Neutron stars do not produce energy but lose the gravitational energy gained during the core collapse by neutrino emission. This cooling determines the slowing down of the rotation motion in pulsars. Neutrinos and anti-neutrinos mainly produced by beta decay and inverse beta decay carry out the energy of the core. This is called the URCA process [Ga41]. Actually, the URCA process is strongly suppressed by energy and momentum conservation unless a minimum amount of protons, around 11% of the baryonic density, is present [La91]. This minimal amount is strongly related to the symmetry energy. It turns out that:

$$\mu_e = \mu_\mu = \mu_n - \mu_p = -\partial E / \partial x \approx 4(1-2x)E_{sym}(\rho), \qquad (75)$$

where $x = \rho_p / \rho$ **is the proton fraction. Eq. (75) is valid for beta-equilibrated matter, where** μ_e, μ_μ, μ_n **and** μ_p **are the electron, muon, neutron and proton chemical potentials, respectively. Eq. (75), together with the charge neutrality condition** $\rho_p = \rho_e + \rho_\mu$, **allows determining the equilibrium proton fraction. This shows how the proton fraction is related to the symmetry energy. Relativistic mean-field models, having typically larger values of the symmetry energy, satisfy the criterium of minumum amount of protons around the saturation density while most of non-relativistic mean-field models do not.**
However, URCA process is too efficient to explain the cooling with time which is observed for several neutron stars. It has been for instance suggested that superfluidity leading to the presence of a neutron pairing gap may quench cooling from the URCA process [Mo07]. A modified URCA process is also considered where adding an additional neutron as a spectator of the process allows momentum and energy conservation. It should be noted that the specific heat of the crust is an important ingredient in the cooling modelization. Specific heat actually depends on the excitation spectrum (vibrations in the crust) which is

different in the superfluid and in the normal phases (pairing correlations would affect the specific heat and, consequently, the cooling time [Mo07]).
A typical example of excitation spectra calculated in an inner-crust Wigner-Seitz cell of neutron stars [NV73] is displayed in Fig. 13 [Gr08] (we refer to P. Pizzochero's Lectures for the details about the Wigner-Seitz modelization of the Coulomb lattice present in the neutron-star crust). This is another example of applications of the EDF models to neutron star physics: the vibrations in the crust are described with the HFB + QRPA approaches and the quadrupole excitation spectrum shown in the figure is calculated for the Wigner-Seitz cell having a radius of 19.6 fm, a number of protons Z = 40 and a number of neutrons N = 1460. A very collective low-energy excitation mode is found. Similar results have also been found for other Wigner-Seitz cells at different baryonic densities in the crust of the star [Kh05].
In Fig. 14 the transition density associated to this collective low-lying mode is displayed showing that the strongest contribution to this excitation comes from the free gas of neutrons located outside the central nuclear cluster of the Wigner-Seitz cell with Z = 40 protons. The nature of this excitation mode is thus very different from that of a low-lying quadrupole excitation mode in a finite nucleus.

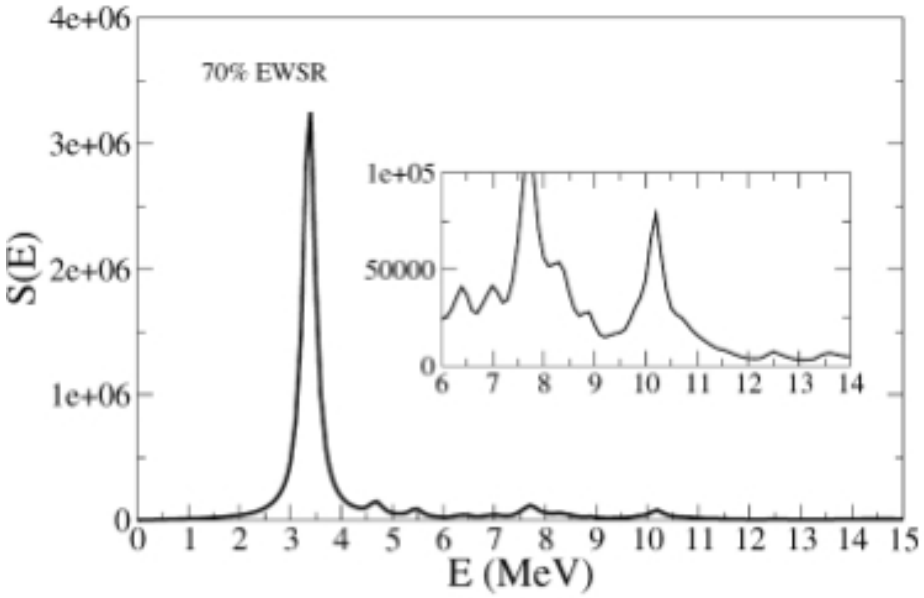

Fig. 13 [Gr08]

Neutron quadrupole QRPA strength distributions for the Wigner-Seitz cell with Z = 40 and N = 1460 (inner crust of a neutron star)

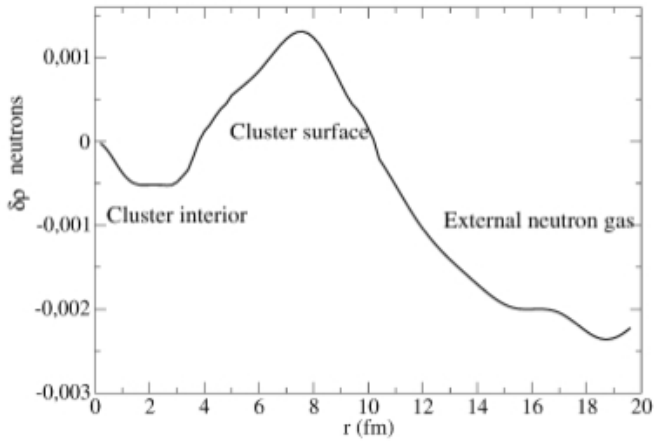

Fig. 14 [Gr08]

Neutron transition density in units of fm^{-3} for the low-energy mode in the Wigner-Seitz cell described in Fig. 13

On the theoretical side, the mass and the radius of a neutron star are determined by solving the hydrostatic equilibrium equation. The equation of state is required for this. It is important noticing that equations of state are typically constrained around the saturation density because the observables used for fitting the parameters are measured in nuclei. In neutron stars, the density ranges from subnuclear densities in the crust up to several times the saturation density in the core. Furthermore, the isospin asymmetry can be as large as 0.95 in the interior of the star. This means that the equations of state are used at densities and isospin asymmetries very different from the values where the fits are done. This is a delicate point related to the predictive power of the models. Several equations of state have been checked (and some of them rejected). In Fig. 15 [LP01] a mass-radius diagram for different equations of state is shown. For notations and futher explanations see Ref. [LP01].

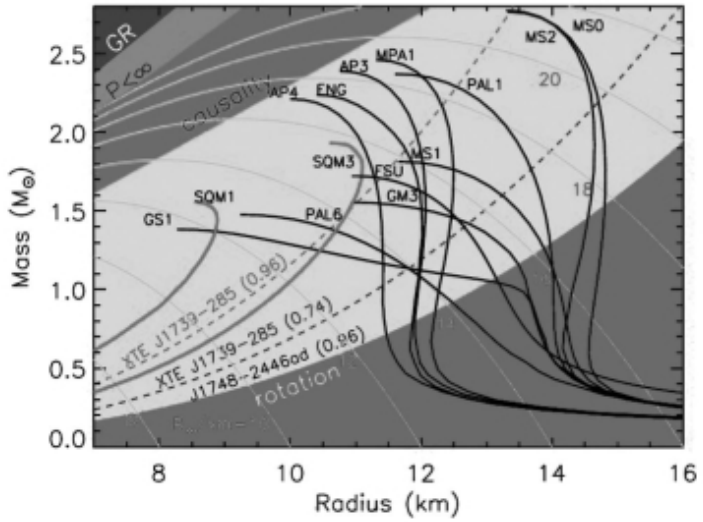

Fig. 15 [LP01]

Mass-radius diagram for different equations of state

XII – APPLICATIONS TO NUCLEAR MATTER. ISOSPIN EFFECTS: ASYMMETRIC MATTER. SPIN INSTABILITIES

Symmetric nuclear matter is an ideal infinite system equally composed of neutrons and protons where the Coulomb interaction is not active. The isospin asymmetry Y_p=Z/A is equal to 0.5. By reducing the value of Y_p, neutron-rich matter is obtained and the value Y_p = 0 characterizes pure neutron matter. An illustration of the equation of state (EoS) of symmetric matter is plotted in Fig. 16 together with examples of EoSs for asymmetric and neutron matter. The differences between the symmetric-nuclear-matter EoSs and the neutron-rich-matter EoSs are typically related to the symmetry energy, which is a crucial quantity for determining the properties of nuclear systems and for the astrophysical implications (as we have seen, for instance, in neutron-star structure and time-evolution).

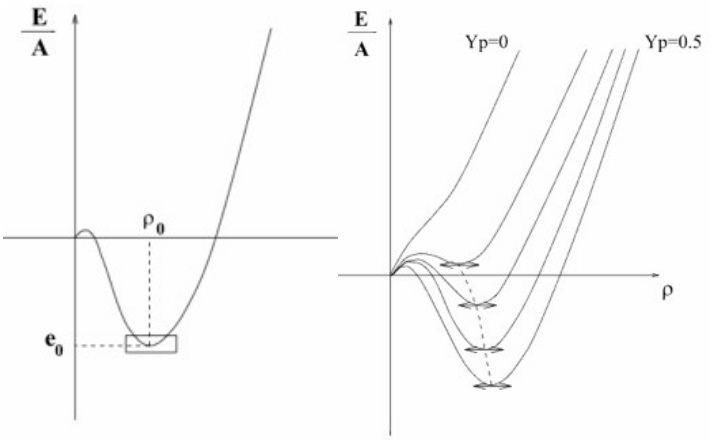

Fig. 16

Left: EoS for symmetric matter. Right: EoSs for symmetric, asymmetric and neutron matter

Different equations of state, different values and density-dependences of the symmetry energy are provided by each theoretical model. This means that each model predicts a specific isospin-dependent and density-dependent behavior for nuclear matter.
In Tables 1 and 2 the properties of infinite nuclear matter obtained with several Skyrme effective forces are shown [Me03].

Force	SIII [15]	Ska [106]	SkM [116]	SGII [124]	SkM* [119]	RATP [122]
ρ_0 (fm^{-3})	0,145	0,155	0,160	0,158	0,160	0,160
k_F (fm^{-1})	1,291	1,320	1,334	1,328	1,333	1,333
r_0 (fm)	1,180	1,154	1,142	1,147	1,143	1,143
a_v (MeV)	–15,851	–15,991	–15,570	–15,794	–15,770	–16,046
K_∞ (MeV)	355,4	263,10	216,6	214,6	216,6	239,51
$(m^*/m)_s$	0,76	0,61	0,79	0,79	0,79	0,67
a_I (MeV)	28,16	32,91	30,03	26,83	30,03	29,26
κ_v (E1 ; T = 1)	0,53	0,94	0,53	0,49	0,53	0,78

Table 1 [Me03]

Properties of nuclear matter obtained with some Skyrme forces

Force	T6 [118]	SkP [35]	SLy4	SLy5	SLy6	SLy7
ρ_0 (fm^{-3})	0,161	0,162	0,160	0,160	0,159	0,158
k_F (fm^{-1})	1,335	1,340	1,333	1,334	1,330	1,328
r_0 (fm)	1,141	1,137	1,143	1,143	1,145	1,147
a_v (MeV)	–15,963	–15,948	–15,969	–15,983	–15,920	15,894
K_∞ (MeV)	235,93	200,96	229,90	229,90	229,80	229,70
$(m^*/m)_s$	1,00	1,00	0,70	0,70	0,69	0,69
a_I (MeV)	29,97	30,00	32,00	32,03	31,96	31,99
κ_v (E1 ; $T = 1$)	0,00	0,35	0,25	0,25	0,25	0,25

Table 2 [Me03]

Properties of nuclear matter obtained with some Skyrme forces

Among these quantities which characterize nuclear matter, we consider here more in detail the saturation density ρ_0, the incompressibility K_∞, the effective mass m^*/m and the symmetry energy a_I. We briefly discuss how these properties are known (from which empirical constraints they are extracted). For a more detailed review, see Ref. [Me03].

XII.A – SYMMETRIC MATTER

The empirical values of the saturation point are known by electron scattering experiments. The saturation density corresponds to the central density of heavy nuclei and its value is independent of the considered nucleus (owing to the saturation properties of the nuclear interaction). In the EoS of symmetric matter, the saturation density is the value associated to the equilibrium point (the minimum point of the curve).
The empirical values associated to the saturation point are:

$\rho_0 = 0.16 \pm 0.002$ fm $^{-3}$

$E/A(\rho_0) = -16.0 \pm 0.2$ MeV

In a Skyrme-mean-field model, the EoS for symmetric matter is written as:

$$\frac{E}{A}(\rho) = \frac{3}{10}\frac{\hbar^2}{m}\left(\frac{3\pi^2}{2}\right)^{2/3}\rho^{\frac{2}{3}} + \frac{3}{8}t_0\rho + \frac{3}{80}\left(\frac{3\pi^2}{2}\right)^{2/3}\Theta_S\rho^{\frac{5}{3}} + \frac{1}{16}t_3\rho^{\alpha+1}, \qquad (76)$$

where:

$$\Theta_S = 3t_1 + t_2(5 + 4x_2). \qquad (77)$$

Thus, each Skyrme parametrization provides slightly different values of ρ_0 and $E/A(\rho_0)$ according to the different values of the parameters in each model.

The incompressibility is the curvature of the EoS at the saturation point. From the Skyrme EoS:

$$K_\infty = 9\rho_0^2\left(\frac{d^2}{d\rho^2}\frac{E}{A}(\rho)\right)_{\rho=\rho_0} = -\frac{3}{5}\frac{\hbar^2}{m}\left(\frac{3\pi^2}{2}\right)^{2/3}\rho_0^{2/3} + \frac{3}{8}\left(\frac{3\pi^2}{2}\right)^{2/3}\Theta_S\rho_0^{5/3} + \frac{9}{16}\alpha(\alpha+1)t_3\rho_0^{\alpha+1}. \quad \textbf{(78)}$$

From theoretical and experimental studies on monopole giant resonances the value of the incompressibility can be extracted. Recently, it has been suggested that pairing could play a role in this context [Kh-1-09]. The commonly accepted values have been extracted from a systematic analysis of Blaizot within the RPA method [Bl80]:

K_∞ = 210 $\pm$ 30 MeV

Nucleons in a nuclear medium (in nuclei or in matter) acquire an effective mass. The effective mass can be defined by the following relation:

$$\varepsilon_p = \frac{\vec{p}^2}{2m} + \Sigma\left(\vec{p}, \varepsilon_p\right) \equiv \frac{\vec{p}^2}{2m*}. \quad \textbf{(79)}$$

This quantity is very important, for instance, for its impact on the level density of nuclei around the Fermi energy. One can write:

$$\frac{\hbar^2}{2m_q^*}\tau_q = \frac{\hbar^2}{2m}\left(\frac{m}{m_q^*}\right)\tau_q$$

From the Skyrme functional:

$$\frac{m}{m_q^*} = 1 + \frac{1}{4}\frac{m}{\hbar^2}\rho\left[t_1(2+x_1) + t_2(2+x_2)\right] + \frac{1}{4}\frac{m}{\hbar^2}\rho_q\left[t_2(1+2x_2) - t_1(1+2x_1)\right]$$

$$= 1 + \frac{1}{4}\frac{m}{\hbar^2}\rho\Theta_V + \frac{1}{4}\frac{m}{\hbar^2}\rho_q\left[\Theta_S - 2\Theta_V\right], \quad \textbf{(80)}$$

with:

$$\Theta_V = t_1(2+x_1) + t_2(2+x_2), \quad \textbf{(81)}$$

The accepted empirical values can be extracted, for instance, by relating this quantity to the isoscalar quadrupole giant resonances:

m*/m = 0.8 - 0.9

XII.B – ASYMMETRIC MATTER AND SYMMETRY ENERGY

The isospin effects can be analyzed in asymmetric matter. The EoS derived from the Skyrme interaction for asymmetric matter is written as:

$$\frac{E}{A}\left(Y_p,\rho\right)=\frac{3}{10}\frac{\hbar^2}{m}\left(\frac{3\pi^2}{2}\right)^{2/3}\rho^{\frac{2}{3}}F_{5/3}$$
$$+\frac{1}{8}t_0\rho\left[2\left(2+x_0\right)-\left(1+2x_0\right)F_2\right]+\frac{1}{48}t_3\rho^{\alpha+1}\left[2\left(2+x_3\right)-\left(1+2x_3\right)F_2\right]$$
$$+\frac{3}{40}\left(\frac{3\pi^2}{2}\right)^{2/3}\rho^{\frac{5}{3}}\left[\Theta_V F_{5/3}+\frac{1}{2}\left(\Theta_S-2\Theta_V\right)F_{8/3}\right], \qquad \textbf{(82)}$$

where:

$$F_m\left(Y_p\right)=2^{m-1}\left[Y_p^m+\left(1-Y_p\right)^m\right]. \qquad \textbf{(83)}$$

As far as the isospin effects are concerned, a very important quantity which strongly characterizes them is the <u>symmetry energy</u> a_I. Its accepted empirical values can be extracted from masses by using models:

$28\ \text{MeV} \le a_I \le 32\ \text{MeV}$

From the Skyrme EoS:

$$a_I=\frac{1}{2}\frac{d^2}{dI^2}\frac{E}{A}\left(I,\rho\right)\Big|_{I=0}$$
$$=\frac{1}{6}\frac{\hbar^2}{m}\left(\frac{3\pi^2}{2}\right)^{2/3}\rho^{2/3}-\frac{1}{8}t_0\left(2x_0+1\right)\rho-\frac{1}{24}\left(\frac{3\pi^2}{2}\right)^{2/3}\left(3\Theta_V-2\Theta_S\right)\rho^{5/3}$$
$$-\frac{1}{48}t_3\left(2x_3+1\right)\rho^{\alpha+1}. \qquad \textbf{(84)}$$

The importance of the density-dependence of the symmetry energy has been underlined several times in this manuscript; some words about this dependence have to be spent. First, it has to be mentioned that some quantities which characterize the properties of nuclear matter are correlated one to the other [Me03]. A study of the correlations among the incompressibility, the saturation density and the symmetry energy {K,ρ_0, a_I}, for insance in the Skyrme case, would allow a better control on some terms of the Skyrme interaction, namely on its density-dependent term (and thus a better control on the density-dependence of the symmetry energy). The density-dependence could be constrained by heavy-ion collision experiments (see Lectures of M.-F. Rivet). One of the objectives of such experiments would also be to enrich the scenario by using neutron-rich exotic ions. The dependence on neutron/proton asymmetry could also be analyzed in this way.
Some suggestions to extract informations about the symmetry energy from the study of collective modes in asymmetric nuclei have been made [Mo01, Re99].
To conclude, we underline again that, in the neutron-star context, the density-dependence of the symmetry energy has a big impact on predictions of masses, radii, URCA process and neutron-star cooling time (see Sec. XI).

XII.C – SPIN INSTABILITIES IN MATTER

In Landau theory of Fermi liquids, nuclear matter properties can be written in terms of the matrix elements of the interaction at the Fermi surface,

$$\left\langle \vec{k}_1\vec{k}_2 \left| V \right| \vec{k}_1\vec{k}_2 \right\rangle = N_0^{-1}\left[F(\theta) + F'(\theta)\tau_1\cdot\tau_2 + G(\theta)\sigma_1\cdot\sigma_2 + G'(\theta)\sigma_1\cdot\sigma_2\tau_1\cdot\tau_2\right]. \qquad (85)$$

The coefficients F, F', G and G' are functions of the angle between $\vec{k}_1$ and $\vec{k}_2$. A multipole expansion provides the Landau-Migdal parameters F_l,F'_l, G_l and G'_l (l = 0 and 1 in the case of a zero-range Skyrme interaction). The stability of the HF solution constrains the values of these parameters and generates sum rules that have to be satisfied. If these requirements are not satisfied instabilities are generated.
As far as spin or ferromagnetic instabilites (the magnetic susceptibility becomes negative) are concerned it has been shown by Margueron and collaborators that they systematically occur, for Skyrme and Gogny effective interactions, at high densities or large isospin asymmetries [Ma01, Ma02]. High densities and large isospin asymmetries actually define the typical scenarios of astrophysical interest in neutron stars and the use of some of these forces in this context may thus become delicate and even inappropriate. Furthermore, an eventual ferromagnetic transition would have a strong impact on the evolution of a protoneutron star via the mean free path of neutrinos which would be equal to zero [Na99].
In Fig. 17 the densities where a ferromagnetic instability occurs as a function of the neutron/proton asymmetry are shown for some effective forces. The figure is extracted from Ref. [Ma02].

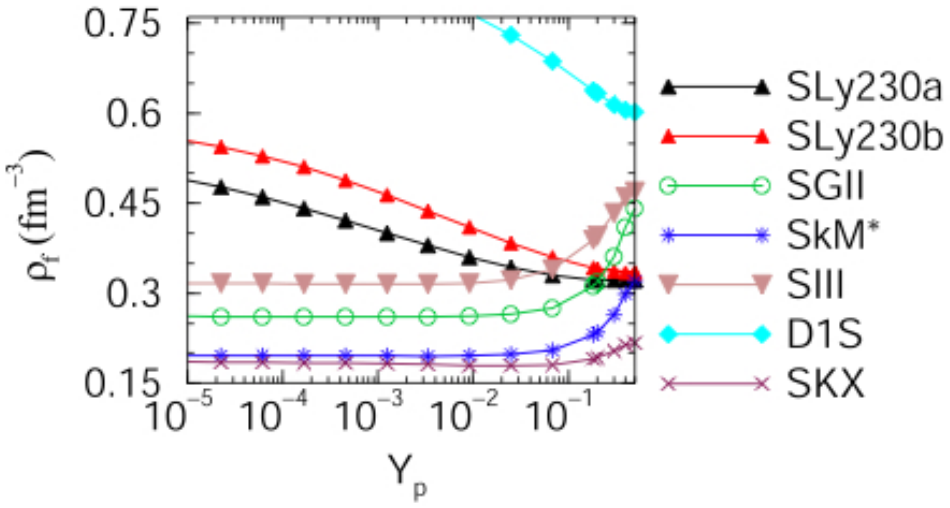

Fig. 17 [Ma02]

Densities where a ferromagnetic instability occurs as a function of the neutron/proton asymmetry for some effective forces

It has to be mentioned that ferromagnetic instabilities are not predicted by microscopic Brueckner-Hartree-Fock calculations with realistic nucleon-nucleon interactions. An illustration of this is shown in Fig. 18 which is extracted from the work of Vidana and collaborators [Vi02].

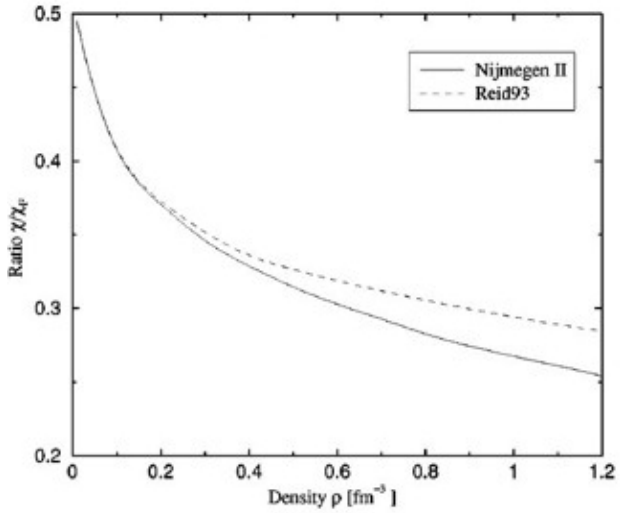

Fig. 18 [Vi02]

Ratio χ/χ_F (where χ is the susceptibility) as a function of the density

A way to cure this kind of instabilities for Skyrme forces has been suggested in Ref. [Ma-1-09] and checked for the ground state of nuclei in [Ma-2-09].
New terms depending on the spin and spin-isospin densities have been added to the Skyrme interaction:

$$V_{new}(\vec{r}_1,\vec{r}_2)=\frac{1}{6}t_3^s\left(1+x_3^s P_\sigma\right)\left[\rho_s(\vec{R})\right]^{\gamma_s}\delta(\vec{r})+\frac{1}{6}t_3^{st}\left(1+x_3^{st}P_\sigma\right)\left[\rho_{st}(\vec{R})\right]^{\gamma_{st}}\delta(\vec{r}), \qquad (86)$$

with the same notation which has already been introduced in Sec. IV. The spin and spin-isospin densities are defined as:

$$\rho_s \equiv \rho_\uparrow - \rho_\downarrow , \qquad (87)$$

$$\rho_{st} \equiv \rho_{n\uparrow} - \rho_{n\downarrow} - \rho_{p\uparrow} + \rho_{p\downarrow} . \qquad (88)$$

XIII – PREDICTIVE POWER WITHIN EDF. PERSPECTIVES

We have addressed several times the issue of the predictive power of the EDF models.
As it has been underlined, these models are constrained to reproduce some properties of known nuclei and to give a reasonable equation of state of matter around the saturation density. Extrapolations to unknown regions of the nuclear chart, to very large isospin asymmetries and to densities very different from the saturation densities are thus not straightforward.
Two aspects have to be considered:

1) the predictive power of the available models in the unexplored regions of the nuclear chart for describing the properties of unstable exotic nuclei;

2) the predictive power of the available models in extreme regions of densities and isospin asymmetries of astrophysical interest.

1) In Fig. 19, the two-proton and two-neutron separation energies for Tin isotopes are displayed (the figure is extracted from the Lectures of D. Lacroix). The pink area represents the region where experimental data are available. It is important to underline that the binding energies of some nuclei are used in the fitting procedures. Large uncertainties are found in the unknown region for the two-neutron separation energies. The prediction for the location of the drip lines is thus a strongly model-dependent result.

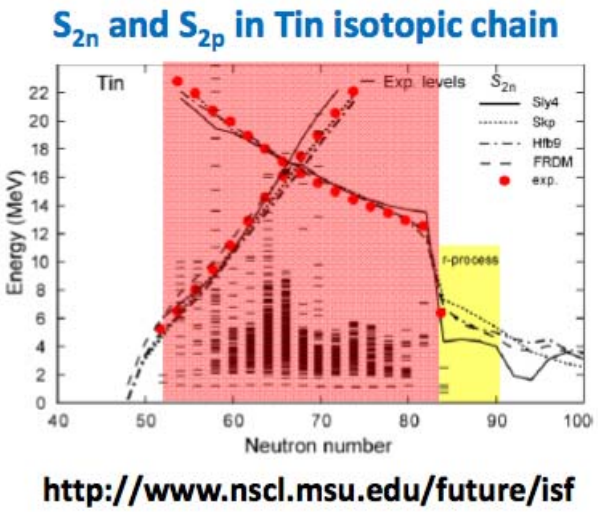

Fig. 19 [La-2-09]

Two-proton and two-neutron separation energies for Tin isotopes. The pink area corresponds to the region where experimental data are available

2) In Fig. 20, the density-dependence of the symmetry energy is shown for different models [St05]. Strong discrepancies are visible far from the saturation point, especially at high densities.

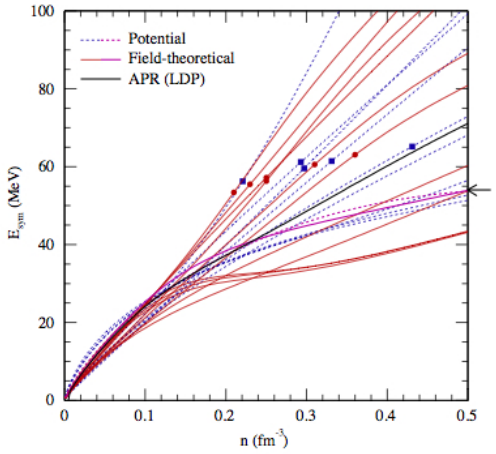

Fig. 20 [St05]

Symmetry energy as a function of the density for different models

1) and 2) are only two illustrations and many other results and analyses could be reported and commented. The conclusion that may be drawn about the predictive power of the EDF models is that the extrapolations in unknown regions have typically very large error bars. The necessity of improving the predictive power is evident and several directions may be followed.
An important contribution is expected from the studies aiming at a more fundamental formulation of the nuclear **interaction** (links with QCD) which should guide in a rigourous way our understanding of the nuclear properties. Also the work on the **functionals** (links with the DFT) is important in the perspectives of building a more global view of the nuclear properties and of using the tools of the DFT in the nuclear framework. The improvement of the available **models** can provide a better description of the nuclear correlations in stable and unstable nuclei. The formulation of more sophisticated beyond-mean-field approaches can thus lead to important advances. Finally, in some cases, the adopted conventional procedures used for fitting the parameters in phenomenological models could be eventually reconsidered. For instance, the **fitting criteria** for the phenomenological interactions could be modified and/or new constraints could be included (this issue is briefly mentioned in the manuscript for the case of the pairing interaction). All these efforts and systematic analysis can provide an implementation of the description of the nuclear many-body problem within the Energy Density Functional theory.

Aknowledgements

I would like to thank Faiçal Azaiez and all the organizers of the École Joliot Curie 2009 for the kind invitation and the very interesting meeting.
I wish to warmly thank Denis Lacroix for his suggestions during the preparation of the Lectures and Michael Bender for a careful reading of the manuscript and his helpful remarks and suggestions.

REFERENCES

[Ad78] S. Adachi and S. Yoshida, Nucl. Phys. A 306 (1978), 53
[An01] M. Anguiano, J.L. Egido, and L.M. Robledo, Nucl. Phys. A 696 (2001), 467
[Ar07] M. Arnould, S. Goriely, and K. Takahashi, Phys. Rep. 450 (2007), 97
[AS08] B. Avez, C. Simenel, Ph. Chomaz, Phys. Rev. C 78, 044318 (2008)
[Au03] G. Audi, A.H. Wapstra, and C. Thibault, Nucl. Phys. A 729 (2003), 337
[AW09] S. Ayik, K. Washiyama, and D. Lacroix, Phys. Rev. C 79 (2009), 054606
[Ba05] F. Barranco, et al., Phys. Rev. C 72 (2005), 054314
[Ba07] B. Bastin, et al., Phys. Rev. Lett. 99 (2007), 022503
[BCS57] J. Bardeen, L.N. Cooper, and J.R. Schrieffer, Phys. Rev. 108 (1957), 1175
[Be79] G.F. Bertsch, P.F. Bortignon, R.A. Broglia, and C.H. Dasso, Phys. Lett. B 80 (1979), 161
[Be80] V. Bernard and N. Van Giai, Nucl. Phys. A 348 (1980), 75
[Be83] G.F. Bertsch, P.F. Bortignon, and R.A. Broglia, Rev. Mod. Phys. 55 (1983), 287
[Be90] H. Bethe, Rev. Mod. Phys. 62 (1990), 801
[Be89] J.F. Berger, M. Girod, D. Gogny, Nucl. Phys. A 502, 85c (1989)
[Be92] D. Beaumel and Ph. Chomaz, Ann. Phys. (N.Y) 213 (1992), 405
[Be04] M. Bender, P. Bonche, T. Duguet, and P.-H. Heenen, Phys. Rev. C 69 (2004), 064303
[Be-1-08] M. Bender, Eur. Phys. J. ST156 (2008) 217-228,
[Be-2-08] M. Bender and P.-H. Heenen, Phys. Rev. C 78 (2008), 024309
[Be-3-08] M. Bender, G. F. Bertsch, and P.-H. Heenen, Phys. Rev. C 78 (2008), 054312
[Be-1-09] M. Bender, Th. Duguet, and D. Lacroix, Phys. Rev. C 79 (2009), 044319

[Be-2-09] G.F. Bertsch, C.A. Bertulani, W. Nazarewicz, N. Schunck, and M.V. Stoitsov, Phys. Rev. C 79 (2009), 034306
[Bl80] J.-P. Blaizot, Phys. Rep. 64 (1980), 171
[Bo90] P. Bonche, et al., Nucl. Phys. A 510 (1990), 466
[Bo01] S.K. Bogner, A. Schwenk, T.T.S. Kuo, G.E. Brown, nucl-th/0111042
[Bo-1-03] S.K. Bogner, T.T.S. Kuo, A. Schwenk, D.R. Entem, and R. Machleidt, Phys. Lett. B 576 (2003), 265
[Bo-2-03] S.K. Bogner, T.T.S. Kuo, and A. Schwenk, Phys. Rep. 386 (2003), 1
[Bo07] L. Bonneau, Ph. Quentin, and K. Sieja, Phys. Rev. C 76 (2007), 014304
[Br99] G. Bruun, Y. Castin, R. Dum, and K. Burnett, Eur. Phys. J. D 7 (1999), 433
[Br00] B.A. Brown, Phys. Rev. Lett. 85 (2000), 5296
[Br05] R.A. Broglia, F. Barranco, P.F. Bortignon, G. Colò, and E. Vigezzi, Nucl. Phys. A 752 (2005), 345
[Br06] A. Brown, et al., Phys. Rev. C 74 (2006), 061303
[BS07] D.M. Brink and Fl. Stancu, Phys. Rev. V 75 (2007), 064311
[Bu02] A. Bulgac and Y. Yu, Phys. Rev. Lett. 88 (2002), 042504
[Ca89] F. Catara, Ph. Chomaz, and N. Van Giai, Phys. Lett. B 233 (1989), 6
[Ca98] F. Catara, M. Grasso, G. Piccitto, and M. Sambataro, Phys. Rev. B 58 (1998), 16070
[Ca06] Klaus Capelle, Brazilian Journal of Physics 36, 1318 (2006)
[Ca08] B.G. Carlsson, J. Dobaczewski, and M. Korteleinen, Phys. Rev. C 78 (2008), 044326
[Ch98] E. Chabanat, P. Bonche, P. Haensel, J. Meyer, and R. Schaeffer, Nucl. Phys. A 635 (1998), 231
[Ch07] F. Chappert, Ph.D. thesis, Univ. Paris Sud, 2007
[Ch08] F. Chappert, M. Girod, S. Hilaire, Phis. Lett. B 668 (2008), 420
[Co01] G. Colò and P.F. Bortignon, Nucl. Phys. A 696 (2001), 427
[Co07] G. Colò, H. Sagawa, S. Fracasso, and P.F. Bortignon, Phys. Lett B 646 (2007), 227
[De80] J. Dechargé, D. Gogny, Phys. Rev. C 21, 1568 (1980)
[De10] J. -P. Delaroche, M. Girod, J. Libert, H. Goutte, S. Hilaire, S. Péru, N. Pillet, and G.F. Bertsch, Phys. Rev. C 81 (2010), 014303
[dG66] P.G. de Gennes, Superconducivity of Metals and Alloys, Perseus Books Publishing, L.L.C., 1966
[Do84] J. Dobaczewski, H. Flocard, and J. Treiner, Nucl. Phys. A 422 (1984), 103
[Do07] J. Dobaczewski, M.V. Stoitsov, W. Nazarewicz, and P.-G. Reinhard, Phys. Rev. C 76 (2007), 054315
[Dr-1-86] S. Drozdz, V. Klent, J. Speth, and J. Wambach, Nucl. Phys. A 451 (1986), 11
[Dr-2-86] S. Drozdz, V. Klent, J. Speth, and J. Wambach, Phys. Lett. B 166 (1986), 18
[Dr90] R.M. Dreizler and E.K.U. Gross, Density Functional Theory, Springer, Berlin, 1990
[Du90] J. Dukelsky and P. Schuck, Nucl. Phys. A 512 (1990), 466
[Du96] J. Dukelsky and P. Schuck, Phys. Lett. B 387 (1996), 233
[Du09] Th. Duguet, M. Bender, K. Bennaceur, D. Lacroix, and Th. Lesinski, Phys. Rev. C 79 (2009), 044320
[Eg04] J. L. Egido and L. M. Robledo, in Extended Density Functionals in Nuclear Physics, edited by G. A. Lalazissis, P. Ring, and D. Vretenar, Lecture Notes in Physics 641 (Springer, Berlin, 2004), p. 269
[En07] J. Engel, Phys. Rev. C 75, (2007), 014306
[Ep09] E. Epelbaum, H.-W. Hammer, and Ulf.G. Meissner, Rev. Mod. Phys. 81 (2009), 1773
[Fi03] P. Finelli, N. Kaiser, D. Vretenar, and W. Weise, Eur. Phys. J. A 17 (2003), 573
[Fi04] P. Finelli, N. Kaiser, D. Vretenar, and W. Weise, Nucl. Phys. A 735 (2004), 449
[Fi06] P. Finelli, N. Kaiser, D. Vretenar, and W. Weise, Nucl. Phys. A 770 (2006), 1
[Fi07] P. Finelli, N. Kaiser, D. Vretenar, and W. Weise, Nucl. Phys. A 791 (2007), 57
[Fio03] C. Fiolhais, F. Nogueira and M Marques (Eds.) A Primer in Density Functional Theory, Springer Lecture Notes in Physics, Vol. 620, 2003

[FW71] A.L. Fetter and J.D. Walecka, Quantum Theory of Many-Particle Systems, San Francisco, Mc Graw-Hill, 1971
[Ga41] G. Gamow and M. Schoenberg, Phys. Rev. 59 (1941), 539
[Ga06] D. Gambacurta, M. Grasso, F. Catara, and M. Sambataro, Phys. Rev. C 73 (2006), 024319
[Ga-1-06] D. Gambacurta, M. Sambataro, and F. Catara, Phys. Rev. C 66 (2006), 014310
[Ga09] D. Gambacurta and F. Catara, Phys. Rev. B 79 (2009), 085403
[Ga-1-09] D. Gambacurta, F. Catara, and M. Grasso, Phys. Rev. C 80 (2009), 014303
[Ga10] D. Gambacurta, M. Grasso, and F. Catara, Phys. Rev. C, in press; arXiv:1002.3563
[Gi-1-08] B. Giraud, et al., Phys. Rev. A 78 (2008), 032507
[Gi-2-08] B. Giraud, Phys. Rev. C 77 (2008), 014311
[Gl97] N.K. Glendenning, Compact Stars, Springer-Verlag, New York (1997)
[Go75] D.Gogny, Proceedings of the International Conference on Nuclear Selfconsistent Fields, Trieste, 1975. G. Ripka and M. Porneuf, Eds. North Holland, Amsterdam, 1975
[Go-1-09] S. Goriely, S. Hilaire, M. Girod, and S. Péru, Phys. Rev. Lett. 102 (2009), 242501
[Go-2-09] S. Goriely, N. Chamel, and J.M. Pearson, Phys. Rev. Lett. 120 (2009), 152503
[Gr00] M. Grasso and F. Catara, Phys. Rev. C 63 (2000), 014317
[Gr02] M. Grasso, F. Catara, and M. Sambataro, Phys. Rev. C 66 (2002), 064303
[Gr03] Marcella Grasso and Michael Urban, Phys. Rev. A 68 (2003), 033610
[Gr07] M. Grasso, Z.Y. Ma, E. Khan, J. Margueron, and N. Van Giai, Phys. Rev. C 76 (2007), 044319
[Gr08] M. Grasso, E. Khan, J. Margueron, and N. Van Giai, Nucl. Phys. A 807 (2008), 1
[Gr09] M. Grasso, E. Khan, and J. Margueron, Proceedings of the Conference NSD09, Dubrovnik, Croatia, May 2009
[GS09] C. Golabek and C. Simenel, Phys. Rev. Lett. 103 (2009), 042701
[Ha64] K. Hara, Prog. Theor. Phys. 32 (1964), 88
[He09] K. Hebeler, Th. Duguet, Th. Lesinski, and A. Schwenk, Phys. Rev. C 80 (2009), 044321
[HK64] P. Hohenberg and W. Kohn, Phys. Rev. 136 (1964), B864
[Ho76] T. Hoshino and A. Arima, Phys. Rev. Lett. 37 (1976), 266
[HP01] C.J. Horowitz and J. Piekarewicz, Phys. Rev. Lett. 86 (2001), 5647
[Hu87] K. Huang, Statistical Mechanics, Wiley, New York, 1987
[Ka93] D. Karadjov, V.V. Voronov, and F. Catara, Phys. Lett. B 306 (1993), 166
[Kh02] E. Khan, N. Sandulescu, M. Grasso, and N. Van Giai, Phys. Rev. C 66 (2002), 024309
[Kh05] E. Khan, N. Sandulescu, and N. Van Giai, Phys. Rev. C 71 (2005), 042801 (R)
[Kh09] E. Khan, M. Grasso, and J. Margueron, Phys. Rev. C 80 (2009), 044328
[Kh-1-09] E. Khan, Phys. Rev. C 80 (2009), 057302
[Kl91] A. Klein, N.R. Walet, and G. Do Dang, Nucl. Phys. A 535 (1991), 1
[Kl08] P. Klupfel, J. Erler, P.-G. Reinhard, and J. A. Maruhn, Eur. Phys. J. A 37 (2008), 343
[Kn76] W. Knupfer and M.G. Huber, Z. Phys. 276 (1976), 99
[Ko06] G. Kotliar, S.Y. Savrasov, K. Haule, V.S. Oudovenko, O. Parcollet, and C.A. Marianetti, Rev. Mod. Phys. 78 (2006), 865
[Ko08] M. Korteleinen, J. Dobaczewski, K. Mizuyama, and J. Toivanen, Phys. Rev. C 77 (2008), 064307
[Kr98] F. Krmpotić, E.J.V. De Passos, D.S. Delion, J. Dukelsky, and P. Schuck, Nucl. Phys. A 637 (1998), 295
[KS65] W. Kohn and L.J. Sham, Phys. Rev. 140 (1965), A1133
[La90] G. Lauritsch and P. G. Reinhard, Nucl. Phys. A 509 (1990), 287; K. Takayanagi, K. Shimizu and A. Arima, Nucl. Phys. A 477 (1988), 205; A. Mariano, F. Krmpotic and A. F. R. de Toledo Piza, Phys. Rev. C49 (1994), 2824
[La91] J.M. Lattimer, C.J. Pethick, M. Prakash, and P. Haensel, Phys. Rev. Lett. 66 (1991), 2701
[La04] D. Lacroix, S. Ayik, and Ph. Chomaz, Prog. Part. Nucl. Phys. 52 (2004), 497

[La09] D. Lacroix, Th. Duguet, and M. Bender, Phys. Rev. C 79 (2009), 044318
[La-2-09] D. Lacroix, contribution to this volume
[Le07] T. Lesinski, M. Bender, K. Bennaceur, T. Duguet, and J. Meyer, Phys. Rev. C 76 (2007), 014312
[Li99] J. Libert, M. Girod, and J.-P. Delaroche Phys. Rev. C 60 (1999), 054301
[Li07] E. Litvinova, P. Ring, and V. Tselyaev, Phys. Rev. C 75 (2007), 064308
[Lo06] W. Long, et al., Phys. Lett. B 640 (2006), 150
[LP00] J.M. Lattimer and M. Prakash, Phys. Rep. 333 (2000), 121
[LP01] J.M. Lattimer and M. Prakash, Astrophys. J. 550 (2001), 426
[Ma67] N.H. March, W.H. Young, and S. Sapanthar, The Many-Body Problem in Quantum Mechanics, Cambridge University Press, 1967
[Ma92] N.H. March, Electron Density Theory of Atoms and Molecules, Academic Press, London, 1992
[Ma01] J. Margueron, Ph.D. thesis, Univ. Paris Sud, 2001
[Ma02] J. Margueron, J; Navarro, and Nguyen Van Giai, Phys. Rev. C 66 (2002), 014303
[Ma08] J. Margueron, H. Sagawa, and K. Hagino, Phys. Rev. C 77, 054309 (2008)
[Ma09] M. Matsuo, COMEX3 Proceedings, June 2009
[Ma-1-09] J. Margueron and H. Sagawa, J. Phys. G 36 (2009), 125102
[Ma-2-09] J. Margueron, S. Goriely, M. Grasso, G. Colò, and H. Sagawa, J. Phys. G 36 (2009), J. Phys. G 36 (2009), 125103
[Me03] J. Meyer, Ann. Phys. Fr. 28, n. 3, 2003
[Me09] J. Messud, M. Bender, and E. Suraud, Phys. Rev. C 80 (2009), 054314
[Mo01] K. Morawetz, U. Fuhrmann, R. Walke, Isospin Physics in Heavy-Ion Collisions at Intermediate Energies, edited by Bao-An Li, W.U. Schroeder (Nova Science Pub. Inc., New York, 2001)
[Mo07] Ch. Monrozeau, J. Margueron, and N. Sandulescu, Phys. Rev. C 75 (2007), 065807
[Na99] J. Navarro, E.S. Hernández, and D. Vautherin, Phys. Rev. C 60 (1999), 045801
[Ne82] J.W. Negele, Rev. Mod. Phys. 54 (1982), 913
[Ni95] S. Nishizaki and J. Wambach, Phys. Lett. B 349 (1995), 7
[Ni98] S. Nishizaki and J. Wambach, Phys. Rev. C 57 (1998), 1515
[Ni-1-06] T. Nikšic, D. Vretenar, and P. Ring, Phys. Rev. C 73 (2006), 034308
[Ni-2-06] T. Nikšic, D. Vretenar, and P. Ring, Phys. Rev. C 74 (2006), 064309
[Ni08] T. Nikšić, D. Vretenar, and P. Ring, Phys. Rev. C 78 (2008), 034318
[Ni09] T. Nikšic, Z. P. Li, D. Vretenar, L. Prochniak, J. Meng, P. Ring, Phys. Rev. C 79 (2009), 034303
[NV72] J.W. Negele and D. Vautherin, Phys. Rev. C 5 (1972), 1472
[NV73] J.W. Negele and D. Vautherin, Nucl. Phys A 207 (1973), 298
[Ot05] T. Otsuka, T. Suzuki, R. Fujimoto, H. Grawe, and Y. Akaishi, Phys. Rev. Lett. 95, 232502 (2005)
[Ot06] Takaharu Otsuka, Toshiaki Matsuo, and Daisuke Abe, Phys. Rev. Lett. 97 (2006), 162501
[Pa89] R.G. Parr and W. Yang, Density-Functional Theory of Atoms and Molecules, Oxford University Press, Oxford, 1989
[Pa-1-09] P. Papakonstantinou and R. Roth, Phys. Lett. B 671 (2009), 356
[Pa-2-09] P. Papakonstantinou and R. Roth, arXiv:0910.1674v1 [nucl-th]
[Pe96] J.P. Perdew, K. Burke, and M. Ernzerhof, Phys. Rev. Lett. 77, 3865 (1996)
[Pe05] John Perdew, et al., The Journal of Chemical Physics 123 (2005), 062201
[Pi08] N. Pillet, J.F. Berger, and E. Caurier, Phys. Rev. C 78 (2008), 024305
[Pr65] J. da Providencia, Nucl. Phys. 61 (1965), 87
[Qu04] Ph. Quentin, et al., Nucl. Phys. A 734 (2004), 477
[Ra98] A.A. Raduta, C. M. Raduta, A. Faessler, and W. A. Kaminski, Nucl. Phys. A 634 (1998), 497
[Re99] P.G. Reinhard, Nucl. Phys. A 649 (1999), 305c
[Ro68] D.J. Rowe, Rev. Mod. Phys. 40 (1968), 153

[Ro02] R. R. Rodriguez-Guzman, J. L. Egido, and L. M. Robledo, Nucl. Phys. A709 (2002), 201
[Ro05] T. R. Rodriguez, J. L. Egido, and L. M. Robledo, Phys. Rev. C 72 (2005), 064303
[Ro10] T. Rodriguez, L. Egido, preprint arXiv:1004.2877
[RS80] P. Ring and P. Schuck, The Nuclear Many-Body Problem, Springer-Verlag Berlin Heidelberg New York, 1980
[Sa95] M. Sambataro and F. Catara, Phys. Rev. C 51 (1995), 3066
[Sa97] M. Sambataro and J. Suhonen, Phys. Rev. C 56 (1997), 782
[Sa99] M. Sambataro and N. Dinh Dang, Phys. Rev. C 59 (1999), 1422
[SAL07] C. Simenel, B. Avez, and D. Lacroix, Joliot-Curie Lectures, 17-22 September 2007
[SB77] Fl. Stancu, D.M. Brink, and H. Flocard, Phys. Lett. B 68 (1977), 168
[Sc-1-84] B. Schwesinger and J. Wambach, Phys. Lett. B 134 (1984), 29
[Sc-2-84] B. Schwesinger and J. Wambach, Nucl. Phys. A 426 (1984), 253
[Sc04] J.P. Schiffer, et al., Phys. Rev. Lett. 92 (2004), 162501
[Si07] K. Sieja, T.L. Ha, Ph. Quentin, and A. Baran, Int. J. Mod. Phys. E 16 (2007), 289
[Sk56] T.H.R. Skyrme, Phil. Mag. 1 (1956), 1043
[Sk59] T.H.R. Skyrme, Nucl. Phys. 9 (1959), 615
[St05] A.W. Steiner, M. Prakash, J.M. Lattimer, and P.J. Ellis, Phys. Rep. 411 (2005), 325
[Ta04] S. Takahara, M. Tohyama, and P. Schuck, Phys. Rev. C 70 (2004), 057307
[TB01] S. Typel and B.A. Brown, Phys. Rev. C 64 (2001), 027302
[Te07] G. Tertychny, V. Tselyaev, S. Kamerdzhiev, F. Krewald, J. Speth, E. Litvinova and A. Avdeenkov, Nucl. Phys. A 788 (2007), 159
[To89] M. Tohyama and M. Gong, Z. Phys. A 332 (1989), 269
[To07] M. Tohyama, Phys. Rev. C 75 (2007), 044310
[VB72] D. Vautherin and D.M. Brink, Phys. Rev. C 5 (1972), 626
[Vo99] C. Volpe, Ph. Chomaz, M.V. Andres, F. Catara, and E. Lanza, Nucl. Phys. A 647 (1999), 246
[Vi02] I. Vidana, et al., Phys. Rev. C 65 (2002), 035804; 66 (2002), 045801
[Ya83] C. Yannouleas, M. Dworzecka, and J.J. Griffin, Nucl. Phys. A 397 (1983), 239
[Ya-1-86] C. Yannouleas, Phys. Rev. C 35 (1986), 1159
[Ya-2-86] C. Yannouleas and S. Jang, Nucl. Phys. A 455 (1986), 40
[Ya09] M. Yamagami, Y.R. Shimizu, and T. Nakatsukasa, Phys. Rev. C 80 (2009), 064301